UNIVERSIDADE ESTADUAL PAULISTA

"JÚLIO DE MESQUITA FILHO"

FACULDADE DE CIÊNCIAS FARMACÊUTICAS

CAMPUS DE ARARAQUARA

PROGRAMA DE PÓS-GRADUAÇÃO EM BIOCIÊNCIAS E BIOTECNOLOGIA APLICADAS À FARMÁCIA

RACHEL TEMPERANI AMARAL MACHADO

"Estudo de caracterização do complexo *tris*-(1,10-fenantrolina)ferro(II) incorporado ao sistema lípidico nanoestruturado e sua atividade anti-*Mycobacterium tuberculosis*"

Araraquara, SP

2021

RACHEL TEMPERANI AMARAL MACHADO

“Estudo de caracterização do complexo *tris*-(1,10-fenantrolina)ferro(II) incorporado ao sistema lípidico nanoestruturado e sua atividade anti-*Mycobacterium tuberculosis*”

Dissertação apresentada ao Programa de Pós-graduação em Biociências e Biotecnologia Aplicadas à Farmácia, área de Biotecnologia, UNESP, como parte dos requisitos para obtenção do Título de Mestre em Biociências e Biotecnologia Aplicadas à Farmácia.

Orientador: Prof. Dr. Fernando Rogério Pavan

Coorientadora: Drª. Patricia Bento da Silva

Araraquara, SP

2021

Machado, Rachel Temperani Amaral.
M149e Estudo de caracterização do complexo tris-(1,10-fenantrolina) ferro (II) incorporado ao sistema lípidico nanoestruturado e sua atividade anti-*Mycobacterium tuberculosis* / Rachel Temperani Amaral Machado. – Araraquara: [S.n.], 2021.
62 f. : il.

Dissertação (Mestrado) – Universidade Estadual Paulista. "Júlio de Mesquita Filho". Faculdade de Ciências Farmacêuticas. Programa de Pós Graduação em Biociências e Biotecnologia Aplicadas à Farmácia. Área de concentração: Biotecnologia.

Orientadora: Fernando Rogério Pavan.
Coorientadora: Patricia Bento da Silva.

1. *Mycobacterium tuberculosis*. 2. Fenantrolina. 3. Tris1. 4. 10-fenantrolina ferro(II). 5. Sistema lipídico nanoestruturado. 6. Novos antibióticos. I. Pavan, Fernando Rogério, orient. II. Silva, Patricia Bento da, coorient. III. Título.

Diretoria do Serviço Técnico de Biblioteca e Documentação - Faculdade de Ciências Farmacêuticas
UNESP - Campus de Araraquara

CAPES: 33004030081P7
Esta ficha não pode ser modificada

CERTIFICADO DE APROVAÇÃO

TÍTULO DA DISSERTAÇÃO: Estudo de caracterização do complexo tris-(1,10-fenantrolina)ferro(II) incorporado ao sistema lipídico nanoestruturado e sua atividade anti-*Mycobacterium tuberculosis*

AUTORA: RACHEL TEMPERANI AMARAL MACHADO
ORIENTADOR: FERNANDO ROGERIO PAVAN
COORIENTADORA: PATRÍCIA BENTO DA SILVA

Aprovada como parte das exigências para obtenção do Título de Mestra em BIOCIÊNCIAS E BIOTECNOLOGIA APLICADAS À FARMÁCIA, área: Análises Clínicas pela Comissão Examinadora:

Prof. Dr. FERNANDO ROGERIO PAVAN (Participaçao Virtual)
Departamento de Ciencias Biologicas / Faculdade de Ciencias Farmaceuticas UNESP Araraquara

Prof. Dr. ROBERTO SANTANA DA SILVA (Participaçao Virtual)
Departamento de Física e Química / Faculdade de Ciências Farmacêuticas - USP - Ribeirão Preto

Prof. Dr. MARLUS CHORILLI (Participaçao Virtual)
Departamento de Fármacos e Medicamentos / Faculdade de Ciências Farmacêuticas - UNESP - Araraquara

Araraquara, 25 de outubro de 2021

Agradecimentos

Aos meus pais, Flavio e Rosangela e a minha irmã Larissa que nunca mediram esforços para me apoiar e me fazer feliz.

A Camila, minha noiva. Obrigada por todo o amor, paciência, cooperação, incentivo e ativa participação em todos os momentos de minha vida.

A todos os meus amigos e colegas de laboratório e da pós-graduação, pelo apoio, suporte e ensinamento. Agradeço por todos os nossos momentos compartilhados, sendo estes difíceis ou alegres.

Ao meu orientador, Prof. Dr. Fernando Rogério Pavan, por toda sua dedicação e pela confiança e liberdade a mim concebidos para o desenvolvimento deste trabalho.

A minha coorientadora, Drª Patrícia Bento da Silva, por ser durante todos esses anos o meu "porto seguro científico", com toda sua paciência, seu companheirismo, sua dedicação e conhecimento.

Ao CNPQ processo: 130612/2019-7 e à Fundação de Amparo à Pesquisa do Estado de São Paulo (FAPESP), processo: 2019/10326-7, pelo apoio financeiro para a realização deste trabalho, sem o qual para mim este sonho não seria possível.

Ao programa de Biociências e Biotecnologia Aplicadas à Farmácia de UNESP-AQA e à Faculdade de Ciências Farmacêuticas UNESP de Araraquara, o local que com muito orgulho e honra considero minha casa.

“O primeiro dever da inteligência é desconfiar dela mesma.” - Albert Einstein

Resumo

A tuberculose (TB), apresenta cerca de 10 milhões de casos por ano em todo o mundo. Além disso, as elevadas taxas de resistência às principais classes de antimicrobianos contribuem para que a TB se encontre entre os maiores causadores de morte por um agente infeccioso. Sendo assim, faz-se evidente a necessidade de controle e combate dessa doença que representa uma séria ameaça à saúde pública global. Para tanto, é preciso enfrentar o desafio do desenvolvimento de novos agentes ativos contra a TB. Nesse trabalho, o complexo metálico tris-(1,10-fenantrolina)ferro(II) ($[Fe(fen)_3]^{2+}$), foi selecionado para o estudo, visto que trabalhos anteriores do nosso grupo demonstraram que este complexo é um bom candidato contra TB. Além disso, quando incorporado a um sistema lipídico nanoestruturado (SLN) demonstrou boa biodisponibilidade oral. Diante desses fatos, o objetivo deste trabalho foi caracterizar o complexo incorporado ao SLN e verificar sua atividade anti-*Mycobacterium. tuberculosis*. A frequência de resistência do *Mycobacterium tuberculosis* a $[Fe(fen)_3]^{2+}$ é menor do que a de outros fármacos de primeira linha para o tratamento da tuberculose, como a rifampicina. Ele se mostrou específico na inibição de micobactérias. Foi possível obter sistemas lipídicos nanoestruturados constituídos de colesterol como fase oleosa, fosfatidilcolina de soja, oleato de sódio e Eumulgin® HRE 40 [óleo de rícino de polioxil 40 hidrogenado]; na proporção de 3: 6: 8, como tensoativo e tampão-fosfato pH 7,4 como fase aquosa (SLN) e incorporar com sucesso o complexo $[Fe(fen)_3]^{2+}$ ao mesmo (SLN+($[Fe(fen)_3]^{2+}$)). A formulação de SLN+$[Fe(fen)_3]^{2+}$ revelou-se estável por até 90 dias a 5ºC e também se apresentam estáveis após 24h em soluções de pHs que remetem os encontrados no estômago e no sangue, e em contato com meios de cultura utilizados em outras metodologias *in vitro*, comprovando a integridade das partículas durante estes ensaios. O SLN mostrou uma taxa de eficiência de encapsulamento próxima a 60% de $[Fe(fen)_3]^{2+}$. Partículas de SLN+$[Fe(fen)_3]^{2+}$ mostraram-se homogêneas (PdI = 0,17), apresentando carga superficial negativa de -34,7mV e tamanho médio de 163nm, definido pela técnica de espalhamento dinâmico de luz (DLS) e confirmado por microscopia eletrônica de transmissão (TEM), que também revelou sua morfologia esférica. $[Fe(fen)_3]^{2+}$ apresentou um valor de CIM_{90} de 4,17 µM na sua forma livre e 23,39 µM quando incorporado no SLN. Estudos futuros devem analisar o perfil de liberação *in vitro*, a atividade *in vivo* e segurança do SLN+$[Fe(fen)_3]^{2+}$ para entender se esta combinação tem potencial para prosseguir como candidato a contra a tuberculose.

Palavras-chave: *Mycobacterium tuberculosis*, fenantrolina, *tris1,10-fenantrolina ferro (II)*, sistema lipídico nanoestruturado, novos antibióticos.

Abstract

Tuberculosis (TB) presents about 10 million cases per year worldwide. In addition, the high rates of resistance to the main classes of antimicrobials contribute to TB being among the biggest killers of an infectious agent. Thus, the need to control and combat this disease, which represents a serious threat to global public health, is evident. Therefore, it is necessary to face the challenge of developing new agents active against TB. In this work, the metallic complex tris-(1,10-phenanthroline)iron(II) ($[Fe(phen)_3]^{2+}$) was selected for the study, as previous works by our group demonstrated that this complex is a good candidate against TB. Furthermore, when loaded into a nanostructured lipid system (NLS) it demonstrated good oral bioavailability. Given these facts, the objective of this work was to characterize the complex incorporated into NLS and verify its anti-*Mycobacterium tuberculosis* activity. The frequency of resistance of *Mycobacterium tuberculosis* to $[Fe(phen)_3]^{2+}$ is lower than that of other first-line drugs for the treatment of tuberculosis, such as rifampicin. It has been shown to be specific in inhibiting mycobacteria. It was possible to obtain NLS consisting of cholesterol as the oil phase, soy phosphatidylcholine, sodium oleate and Eumulgin® HRE 40 [polyoxyl 40 hydrogenated castor oil]; in a ratio of 3: 6: 8, as surfactant and phosphate-buffer pH 7.4 as aqueous phase, and successfully load the complex $[Fe(phen)_3]^{2+}$ to it (NLS+$[Fe(phen)_3]^{2+}$). The NLS+$[Fe(phen)_3]^{2+}$ formulation proved to be stable for up to 90 days at 5°C and are also stable after 24 hours in solutions with pHs that match those found in the stomach and blood, and in contact with means of culture used in other in vitro methodologies, proving the integrity of the particles during these assays. NLS showed a entrapment efficiency rate close to 60% of $[Fe(phen)_3]^{2+}$. NLS+$[Fe(phen)_3]^{2+}$ particles were homogeneous (PdI = 0.17), with a negative surface charge of -34.7mV and average size of 163nm, defined by the dynamic light scattering (DLS) technique and confirmed by transmission electron microscopy (TEM), which also revealed its spherical morphology. $[Fe(phen)_3]^{2+}$ had a MIC_{90} value of 4.17 µM in its free form and 23.39 µM when incorporated into NLS. Future studies must analyze the in vitro release profile, and the *in vivo* activity and safety of NLS+$[Fe(phen)_3]^{2+}$ in order to fully understand whether this combination of the $[Fe(phen)_3]^{2+}$ and the NLS has the potential to proceed as a drug candidate against TB.

Key words: *Mycobacterium tuberculosis*, phenanthroline, tris 1,10-phenantroline iron (II), new antibiotics

Lista de Siglas e Abreviaturas

$[Fe(fen)_3]^{2+}$	tris-(1,10-fenantrolina)ferro(II)
$[Fe(phen)_3]^{2+}$	tris-(1,10-phenantrolin)iron(II)
ATR	Attenuated total reflectance
BCG	Bacilo Calmette-Guérin
bipi	Bipiridina
CIM	Concentração Inibitória Mínima
COVID-19	Coronavirus disease 2019
DLS	Dynamic Light Scattering
DL%	Drug loading capacity
DMEM	Dulbecco's Modified Eagle's Medium
DMSO	Dimethylsulfoxide
EE%	Entrapment efficiency
EMA	Agência Europeia de Medicamentos
ETB	etambutol, ethambutol
FDA	Food and Drug Administration
Fe	Ferro, Iron
fen	Fenantrolina
FTIR	Fourier Transform Infrared
HIV	Vírus da imunodeficiência humana
ICP-Ms	Inductively Coupled Plasma Mass Spectrometrometry
INH	isoniazida, isoniazid
IPD	Índice de Polidispersão
LOD	Limit of detection
MIC	Minimum inhibitory concentration
NLS	Nanostructured lipid system

NLS+$[Fe(phen)_3]^{2+}$	tris-(1,10-phenantrolin)iron(II) loaded into the Nanostructured lipid system
OADC	Suplemento de meio de cultura, a base de ácido oleico, albumina, dextrose e catalase; oleic acid, albumin, dextrose and catalase
OMS	Organização Mundial da Saúde
PdI	Polydispersity index
PNCT	Programa Nacional de Controle da Tuberculose
PZ	Potencial Zeta
PZA	pirazinamida, pyrazinamide
REMA	Resazurin Microtiter Assay
RIF	rifampicina, rifampicin
SARS-CoV-2	Síndrome respiratória aguda grave coronavírus 2
SIDA	Síndrome da Imunodeficiência Adquirida
SLN	Sistema Lipídico Nanoestruturado
TB	Tuberculose, Tuberculosis
TB-MDR	Tuberculose multidroga resistente
TB-XDR	Tuberculose extensivamente resistente
TEM	Transmission electron microscope
UFC	Unidades formadoras de colônia
ZP	Zeta Potential
Z average	Mean particle size

Lista de Figuras

Capítulo I

Capítulo II

Lista de Tabelas

Capítulo II

Sumário

Capítulo I

1. INTRODUÇÃO

1.1 Tuberculose: Dados gerais, epidemiologia e tratamento

A tuberculose (TB) é uma das doenças mais antigas do mundo. Evidências encontradas em múmias egípcias datadas de 2400 a.C. revelaram deformidades esqueléticas típicas da tuberculose (BARBERIS et al., 2017). Apesar de sua origem antiga, ainda hoje ela representa um grande desafio para a saúde pública mundial. É uma doença infectocontagiosa causada pelo complexo *Mycobacterium tuberculosis* (*Mycobacterium tuberculosis, Mycobacterium africanum, Mycobacterium bovis, Mycobacterium caprae, Mycobacterium microti, Mycobacterium pinnipedii e Mycobacterium canettii*) (ZUMLA; NAHID; COLE, 2013). Sendo o *M. tuberculosis* sua principal espécie causadora, identificada pelo alemão Robert Koch, em 1882. Embora afete comumente os pulmões, também pode afetar outros órgãos sendo então denominada TB extrapulmonar (PAI et al., 2016).

Em geral, a transmissão da doença ocorre quando indivíduos sadios entram em contato com gotículas (aerossóis) expelidas por indivíduos infectados pelo bacilo em sua forma ativa, através da tosse, espirros ou fala, por exemplo. Somente uma pequena taxa de indivíduos que foram expostos, cerca de 5 a 10 %, desenvolverão a doença. No entanto, a probabilidade de desenvolver TB é muito maior entre aqueles coinfectados com o vírus da imunodeficiência humana (HIV), também é maior entre as pessoas afetadas por fatores de risco como desnutrição, diabetes, tabagismo e consumo de álcool (WORLD HEALTH ORGANIZATION, 2020a).

Os indivíduos expostos ao bacilo que não desenvolvem a doença apresentam resposta imune celular eficaz para conter a infecção, e então o *M. tuberculosis* pode assumir o estado de latência (WARD; HOYE; TALAAT, 2008). O processo de TB latente ocorre quando nos pulmões, macrófagos fagocitam os bacilos, esse processo induz uma resposta pró-inflamatória com o recrutamento de mais macrófagos, linfócitos T, plasmócitos e fibroblastos, iniciando a formação do granuloma. Nesse complexo a bactéria permanece em um estado não-replicante (dormente), considerado não infeccioso e que pode permanecer assim por anos. No entanto, à medida que a imunidade diminui, através do envelhecimento ou da imunossupressão, os bacilos dormentes podem ser reativados, o que resulta no desenvolvimento da

forma ativa da TB no indivíduo, que muitas vezes ocorre décadas após a infecção inicial (RUSSELL, 2007).

A Organização Mundial da Saúde (OMS) estima que houve cerca de 10 milhões de casos de TB no mundo em 2019. Deste total 1,4 milhão vieram a óbito em decorrência da doença, dos quais 208.000 mortes correspondem a coinfecções TB-HIV. As coinfecções de TB e HIV recebem grande atenção pois a interação entre as duas doenças apresenta altas taxas de morbidade e de mortalidade, chegando a ser nomeada como “dueto maldito”. Nos dias atuais outra infecção que é capaz de recordar esse dueto, junto com a TB, é a da síndrome respiratória aguda grave coronavírus 2 (SARS-CoV-2) causadora da COVID-19 (coronavirus disease 2019) (VISCA et al., 2021). Mais evidências são necessárias para compreender o potencial da COVID-19 em impactar na reativação de bacilos em estado de latência, por exemplo. Mas alguns autores já trazem a discussão de que a imunossupressão causada pela própria doença ou pelo uso de medicamentos durante o tratamento da COVID-19 poderão impactar futuramente neste quesito (CRISAN-DABIJA et al., 2020; SILVA et al., 2021; YANG; LU, 2020). A pandemia de COVID-19 poderá afetar drasticamente a carga global tuberculose nos próximos anos, aumentando o número de mortes em decorrência da doença já que em muitos locais os serviços de saúde apresentam-se sobrecarregados diminuindo os números de detecção e tratamentos de TB. A estimativa da OMS é de que houveram 1,8 milhões de mortes por TB em 2020 no mundo (WORLD HEALTH ORGANIZATION, 2020a).

O Brasil encontra-se entre os 30 países que juntos, concentram 87% dos casos da doença no mundo. Nos últimos anos o país encontra-se em uma tendência de alta no número de incidência de casos. No ano de 2019, foram notificados 96mil novos casos e 4,9 mil mortes por esta patologia, além de mais 1,8 mil mortes entre os portadores de HIV (WORLD HEALTH ORGANIZATION, 2020a). No país, geralmente a doença está relacionada com as más condições de moradia, nutrição e saneamento básico, ao uso e abuso de álcool, drogas ilícitas e às doenças imunossupressoras, como a Síndrome da Imunodeficiência Adquirida (SIDA) afetando, principalmente, as periferias urbanas, como as favelas e as áreas degradadas dos grandes centros (MINISTÉRIO DA SAÚDE BRASIL, 2017).

A única vacina licenciada para prevenção da tuberculose é a BCG ou bacilo Calmette-Guérin. A BCG foi desenvolvida há quase 100 anos e previne formas graves de TB em crianças, sendo amplamente utilizada. Atualmente, não existe uma vacina

eficaz na prevenção da doença em adultos, embora os resultados de um estudo de fase II do candidato M72/AS01$_E$ sejam promissores (VAN DER MEEREN et al., 2018).

O tratamento de novos casos de TB suscetível no Brasil conta com um esquema terapêutico de duas fases (Figura 1), fase intensiva (Fig 1a) e fase de manutenção (Fig 1b). Segundo o Programa Nacional de Controle da Tuberculose (PNCT), na fase intensiva, que corresponde a um período de dois meses, são administrados por via oral a combinação de quatro fármacos de primeira-linha, rifampicina (RIF), isoniazida (INH), etambutol (ETB) e pirazinamida (PZA). Após este período, inicia-se a fase de manutenção, em que se utiliza apenas RIF e INH por mais quatro meses de tratamento (MINISTÉRIO DA SAÚDE BRASIL, 2017; WORLD HEALTH ORGANIZATION, 2016).

A Fase de manutenção pode se estender por mais 3 meses, totalizando 7 meses, em casos em que o paciente possui um maior risco de recidiva como, por exemplo, no caso de HIV positivos, imunossupressão, diabéticos insulinodependentes, fumantes etc. Os quatro fármacos utilizados no esquema terapêutico padrão desde o ano de 2009, possuem mecanismos de ação diferentes, fator que contribuiu para uma grande diminuição no tempo de tratamento, que até a década de 60 era de 18 meses de duração (RABAHI et al., 2017).

Figura 1. Esquema terapêutico para TB suscetível aos fármacos.

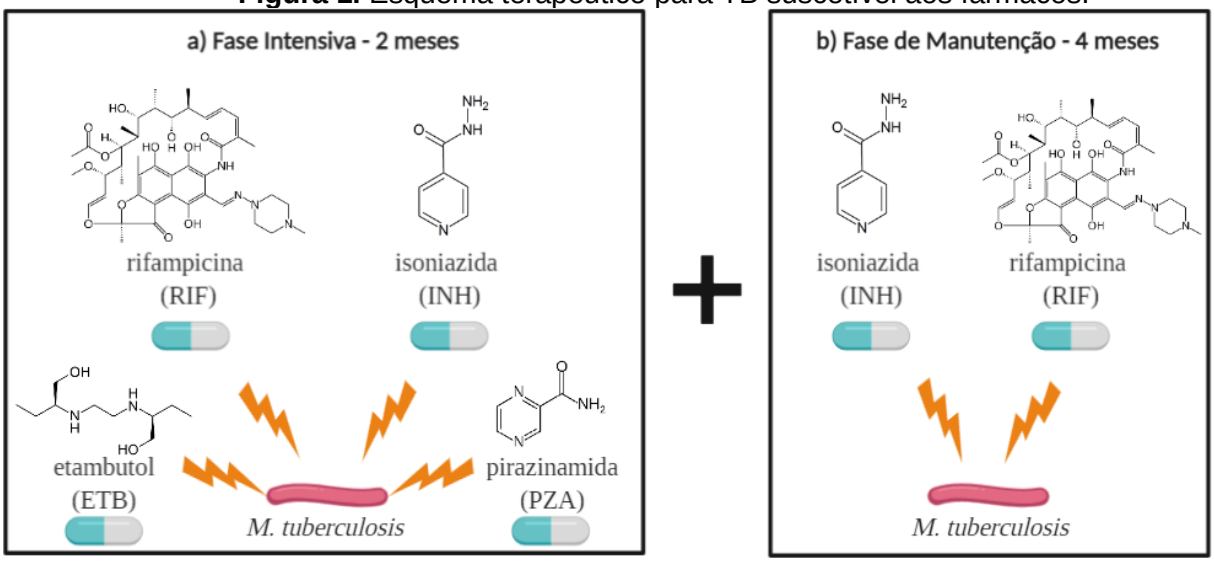

Fonte: Autora

A RIF age inibindo a elongação do RNA durante o processo de transcrição impedindo a síntese de proteínas das células da micobactéria. A PZA ainda não possui seu mecanismo de ação completamente desvendado, mas sabe-se que seu

metábolito ativo, o àcido propiônico reduz o pH intramacrofágico impedindo o crescimento dos bacilos. Os fármacos INH e ETB inibem a formação da parede celular das células das micobacterias impedindo a formação de dois dos principais constituintes da mesma, que são os acídos micolicos e arabinogalactanos, respectivamente. A INH, fármaco específico em inibir micobacterias, é um profármaco que quando ativado pela ennzima KatG gera espécies reativas de oxigênio que impedem a formação dos ácidos micólicos. Enquanto o ETB possui como alvo a arabinosil transferase interrompendo a formação da camada de arabinogalactano (SHETYE; FRANZBLAU; CHO, 2020).

Quando o tratamento de primeira-linha se mostra ineficaz devido à resistência do bacilo aos fármacos, realiza-se o tratamento com fármacos de segunda-linha por exemplo, pertencentes ao grupo de aminoglicosídeos injetáveis e ao grupo de fluoroquinolonas.

A TB multidroga resistente (TB-MDR) é definida como a resistência do bacilo aos dois principais fármacos de primeira-linha, INH e RIF. Uma nova definição da Organização Mundial da Saúde, é a forma de pré resistência estendida (Pré-TB-XDR) que se caracteriza pela resistência a INH e RIF somada a qualquer uma das fluoroquinolonas. Já a forma de resistência estendida (TB-XDR) atende a definição de Pré-TB-XDR além de também ser resistente a um dos fármacos de segunda-linha, bedaquilina ou linezolida (WORLD HEALTH ORGANIZATION, 2021). Somente no ano de 2019 a estimativa foi de 465.000 casos com apenas 38% destes casos recebendo o tratamento adequado (figura 2), 182.000 mortes causadas por TB-MDR e o relato de TB-XDR em 128 países (WORLD HEALTH ORGANIZATION, 2020).

Figura 2. Estimativa da OMS de números de casos de tuberculose resistente aos fármacos e porcentagem de tratamento em 2019.

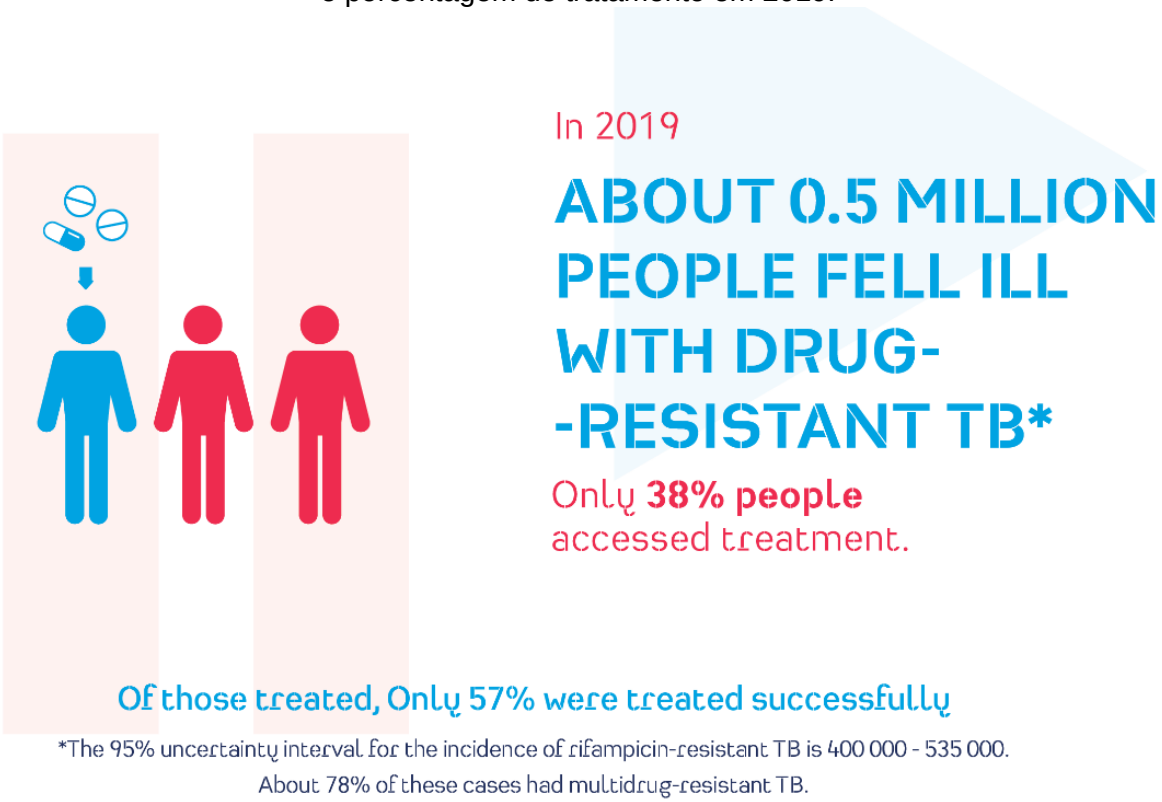

Fonte: https://www.who.int/campaigns/world-tb-day/world-tb-day-2021/campaign-materials

O regime de tratamento para TB-MDR é mais longo e requer fármacos mais caros e mais tóxicos. Para a maioria dos pacientes com TB-MDR, as taxas de sucesso do tratamento são muito menores do que aqueles para a TB suscetível a fármacos (WORLD HEALTH ORGANIZATION, 2020).

Em 2013, dois novos fármacos (bedaquilina e delamanida) foram aprovados pela Food and Drug Administration (FDA) dos EUA e pela Agência Europeia de Medicamentos (EMA) para uso na terapia anti-TB (MAHAJAN, 2013; RYAN; LO, 2014). No entanto, eles receberam apenas uma aprovação regulatória condicional, sendo reservados para os casos de TB-MDR e utilizados na terceira linha de tratamento.

Uma das maiores dificuldades encontradas na cura da TB é a baixa adesão ao tratamento, que por ser muito longo, com muitos fármacos e efeitos adversos, acaba gerando uma desistência de aproximadamente 17% das pessoas. Outro problema enfrentado é a alta resistência aos fármacos já existentes para TB. O fato de pessoas

não concluírem o tratamento, contribui ainda mais para o aumento da resistência bacteriana (COUTO et al., 2014; SILVA et al., 2014).

Em 2017 a OMS destacou, em seu relatório anual, o *M. tuberculosis* como um patógeno prioritário para a pesquisa e desenvolvimento contínuo de novos antibióticos (WORLD HEALTH ORGANIZATION, 2016). Já que as tecnologias empregadas para prevenir, diagnosticar e tratar a TB foram desenvolvidas no século XX, e o patógeno continua a evoluir e desenvolver padrões de resistência complexos para os fármacos disponíveis na terapia, torna-se evidente a necessidade de desenvolver agentes contra a tuberculose mais novos, potentes e seguros que possuam um novo mecanismo de ação sendo capazes de inibir bacilos resistentes aos fármacos e que sejam potencialmente efetivos em bactérias intracelulares e não replicantes, otimizando o atual tratamento da TB (VASAVA et al., 2017; WELLINGTON; HUNG, 2018).

1.2 *tris*-(1-10-fenantrolina)ferro(II)

O uso de metais e complexos metálicos como fármacos em terapias vem crescendo e se tornando cada vez mais importante ao longo das últimas décadas, além do notável sucesso de fármacos anticâncer, como cisplatina, carboplatina e oxaliplatina, os complexos metálicos também mostraram resultados promissores no tratamento de uma variedade de doenças como: diabetes, úlcera, artrite reumatoide, doenças inflamatórias, infecciosas, cardiovasculares etc. (BHARTI; SINGH, 2009).

O ferro (Fe) está entre os elementos de transição mais abundantes na Terra e é um dos micronutrientes essenciais amplamente utilizado por quase todos os organismos vivos para realizar uma grande quantidade de processos bioquímicos. É considerado como um elemento-traço, levando esse nome por estar presente no organismo em pequenas concentrações, porém realizando um papel indispensável nos processos fisiológicos e metabólicos nos seres vivos (WADA, 2004). Esse metal possui a capacidade de formar complexos de grande estabilidade nos estados bi e trivalente (ZHANG; SEN; GIEDROC, 2020).

O nitroprussiato de sódio, é um exemplo de fármaco que contém ferro, bem conhecido e estabelecido na terapia. É um sal de sódio com um complexo de fe^{2+} e oxido nítrico que vem sendo utilizado como um vasodilatador e regulador de pressão arterial por mais de 40 anos (HOTTINGER et al., 2014).

Como demonstrado em estudos anteriores, diferentes complexos com o íon Fe apresentam atividade antimicobacteriana. Em um desses estudos, complexos de Fe (II) e Fe (III) com 3-aminoquinoxalina-2-carbonitrila e dióxido como ligantes, foram sintetizados por Tarallo e colaboradores. Estes complexos foram mais ativos frente ao *M. tuberculosis* do que os ligantes sozinhos, apresentando valor de MIC_{90} de 0,78 µg/mL (TARALLO et al., 2010). Outro estudo, realizado por Campos e colaboradores, evidenciou a potencialização da atividade antimicobacteriana de um sal de piridina quando complexado ao Fe (III) passando de 7,20 µM para 1,07 µM, e inclusive inibindo cepas clínicas de TB-MDR e XDR (CAMPOS et al., 2020).

Exibindo uma combinação de ótimas propriedades estruturais e químicas, ligantes como a fenantrolina (fen) e a bipiridina (bipi) tem sido extensivamente estudados por serem quimicamente versáteis. Diversas aplicações terapêuticas foram obtidas através do emprego destes tipos de ligantes em combinação com diferentes metais de transição (GAO et al., 2016). A 1,10-fenantrolina (1,10-fen), a 2,2'-bipiridina (2,2'-bipi) e seus derivados, tanto em coordenação com metais como no seu estado livre, desestruturam o funcionamento de uma grande variedade de sistemas biológicos (MCCANN et al., 2004).

A molécula de 1,10-fen (Figura 3), amplamente utilizada como um ligante em química analítica e de coordenação (IDRISS et al., 1980; KOCH; ACKERMANN, 1992; LORENZO et al., 1998), é planar, rígida, hidrofóbica e heterocíclica e seus átomos de nitrogênio possuem propriedades favoráveis à ligação de cátions. Essas características estruturais determinam sua capacidade de coordenação em relação a íons metálicos (BENCINI; LIPPOLIS, 2010).

Figura 3. Estrutura química da 1,10-fenantrolina.

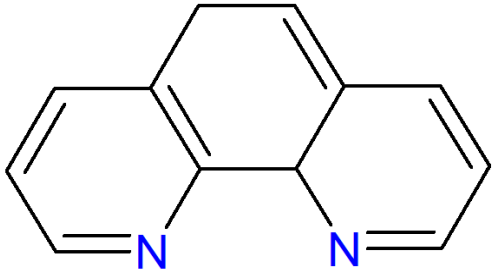

Fonte: autora

Complexos de fen com íons metálicos foram apontados como bactericidas para diferentes gêneros de bactérias e alguns fungos (MCCANN et al., 2004). Em estudos

prévios realizados pelo Laboratório de Pesquisa em Tuberculose da UNESP, a atividade anti-*M. tuberculosis* de diferentes complexos metálicos foi investigada, em especial, complexos de rutênio (II) e fen, que demonstraram atividade promissora contra o *M. tuberculosis in vitro*, sendo observado nesses casos que o complexo como um todo mostrou-se diversas vezes mais ativo que seus ligantes livres (PAVAN et al., 2010, 2011).

A formação do complexo metálico tris-(1,10-fenantrolina)ferro(II), ($[Fe(fen)_3]^{2+}$) mostrado na figura 4, se dá pela complexação do íon de ferro (II) com moléculas de 1-10-fenantrolina. Sua esfera de coordenação é comprovada por estudo de cristalografia (UÇAR et al., 2005). O complexo $[Fe(fen)_3]^{2+}$ tem sido amplamente utilizado como precursor de outras reações químicas já que exibe grande potencial redox. Em relação a sua atividade biológica descrita em literatura, existem relatos de atividade antifúngica (BOTTEGA et al., 2016).

Figura 4. Estrutura química de tris-(1,10-fenantrolina)ferro(II) - ($[Fe(fen)_3]^{2+}$).

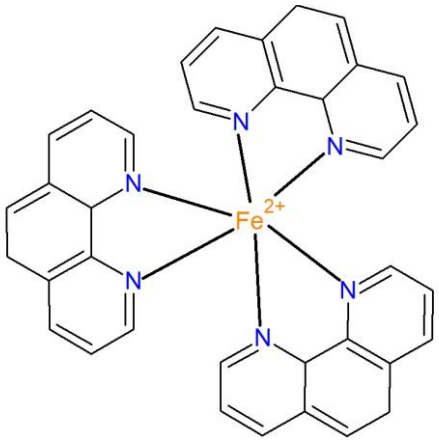

Fonte: autora

1.3 Nanotecnologia Farmacêutica e os Sistema Lipídicos Nanoestruturados

A nanotecnologia pode ser definida como a utilização da tecnologia em moléculas ou estruturas de escala nanométricas para aplicações práticas. O conceito dessa tecnologia foi introduzido em 1959 pelo físico Richard Feynman que descreveu sua ideia de utilizar as máquinas disponíveis para construir máquinas cada vez menores

até a nível molecular (FEYNMAN, 1992). A nanotecnologia é elencada como uma das tecnologias mais promissoras do século 21 (BAYDA et al., 2020).

Abrangendo várias áreas do conhecimento, a nanotecnologia, é uma ciência multidisciplinar que depende da comunhão do conhecimento de áreas como a física, química, biológia e engenharia para sua eficiência (FARIA-TISCHER; TISCHER, 2012). A nanobiotecnologia, surgiu da integração de conhecimentos da biologia, engenharia e da nanociência, e é utilizada para o desenvolvimento de instrumentos e aplicações em sistemas biológicos como diagnósticos, entrega de fármacos (*drug delivery)* e imageamento molecular (KHAN et al., 2015). Essa sub-área do conhecimento tem se intensificado e mostrado excelentes resultados (WEISSIG; PETTINGER; MURDOCK, 2014).

A utilização de nanoestruturas como veículo de moléculas bioativas, vetorização e carregamento de fármacos representa um dos principais objetos de interesse da nanobiotecnologia e da nanotecnologia farmacêutica, e é considerada uma ótima alternativa para contornar propriedades indesejadas de fármacos ou substâncias candidatas, por vezes permitindo o aprimoramento dos mesmos para que possam ser lançadas no mercado ou utilizadas na terapêutica (MAINARDES et al., 2006).

Dentro das sub-área destacada os sistemas nanoestruturados apresentam partículas com dimensões que variam de 10 a 1000 nm, realizando o carreamento de ativos ou fármacos (FONSECA-SANTOS; GREMIÃO; CHORILLI, 2015). Dentre os sistemas nanoestruturados estão os sistemas lipídicos nanoestruturados, que possuem em sua composição lipídios estabilizados por agentes tensoativos. São biocompatíveis e biodegradáveis apresentando estruturas altamente organizadas (OCHEKPE; OLORUNFEMI; NGWULUKA, 2009).

Estes sistemas possuem elevada estabilidade, melhoria da biodisponibilidade do fármaco, e também, podem incorporar substâncias hidrofílicas e hidrofóbicas (PENTENERO, 2017). Além disso, possuem a capacidade de poupar tecidos e células saudáveis, direcionando a molécula ativa ao alvo terapêutico, ofertando a proteção do fármaco contra degradação prematura gerada pelas particularidades inerentes as diferentes vias de administração, e possibilitando a redução nas frequências de dosagem (SAFARI; ZARNEGAR, 2014). Todas essas características podem proporcionar uma melhora na qualidade de vida do paciente e contribuem para a resolução de um importante obstáculo no controle da epidemia de TB que é a baixa adesão ao tratamento (NASIRUDDIN; NEYAZ; DAS, 2017).

Diferentes tipos de sistemas nanocarreadores são promissores para várias vias de administração, abrangendo a administração oral, ocular, parenteral, transdérmica, vaginal e retal (GUPTA; MOULIK, 2008)

A via de administração mais conveniente e amplamente utilizada é a via oral devido à facilidade e aceitação dessa via por parte dos pacientes. No entanto, muitos fármacos possuem baixa dissolução no trato gastrointestinal fator que pode levar a uma redução da biodisponibilidade do mesmo. As ações das enzimas e as variações de pH no trato gastrointestinal também podem afetar o fármaco e sua biodisponibilidade (HOMAYUN; LIN; CHOI, 2019).

Os sistemas do tipo microemulsionado consistem na combinação de dois líquidos imiscíveis, comumente óleo e água, que são estabilizados por tensoativos formando um filme interfacial entre os dois (ABOOFAZELI; LAWRENCE, 1993; CONSTANTINIDES et al., 1994). São sistemas termodinamicamente estáveis e isotropicamente translúcidos com partículas de escala nanométrica que possuem a capacidade de solubilização e proteção dos ativos, melhorando potencialmente a biodisponibilidade oral destes (TENJARLA, 1999).

Os sistemas baseados em nanotecnologia mostraram resultados promissores no tratamento de doenças infecciosas, inclusive TB. O sistema lipídico nanosetruturado (SLN) do tipo microemulsionado utilizado neste trabalho foi desenvolvido e caracterizado em estudos anteriores, com a incorporação de complexos contendo N-óxido e complexos metálicos de rutênio e de cobre, onde resultados promissores foram encontrados no âmbito de atividade contra *M. tuberculosis*, diminuição de citotoxicidade dos complexos e aumento da biodisponibilidade dos mesmos. (DA SILVA et al., 2016, 2018; DE FREITAS et al., 2014; DOS SANTOS FERNANDES et al., 2017).

Além disso, este mesmo sistema foi utilizado em estudo prévio realizado por Solcia et al., em projeto de mestrado realizado no nosso grupo de pesquisa no Laboratório de Pesquisa em tuberculose da UNESP, onde o complexo $[Fe(fen)_3]^{2+}$ mostrou-se como um promissor candidato a fármaco para o tratamento de TB, apresentando eficaz atividade contra micobactérias e quando foi incorporado ao sistema demonstrou estar biodisponível nos plasmas dos animais tratados por via oral após 2h da aplicação e apresentou pico máximo na concentração plasmática em 6h (SOLCIA et al., 2021).

Dos resultados promissores deste último trabalho citado, surgiu a necessidade de estudos mais detalhados sobre o sistema formado com a incorporação do complexo

de ferro ao sistema lipídico em questão (SLN+$[Fe(fen)_3]^{2+}$), na intenção de que este possa ser aplicado de forma oral na terapia, atendendo à necessidade de adesão do paciente no tratamento da tuberculose (WORLD HEALTH ORGANIZATION (WHO), 2016b).

2. OBJETIVOS

2.1 Objetivo Geral

Este projeto teve como objetivo avaliar o complexo tris-(1,10-fenantrolina)ferro(II) quando incorporado ao sistema lipídico nanoestruturado e os possíveis efeitos do complexo de ferro frente a cepa de *Mycobacterium tuberculosis,* H37Rv.

2.2 Objetivos específicos:

- Verificar a frequência de resistência da cepa H37Rv de *M. tuberculosis* em relação ao complexo $[Fe(fen)_3]^{2+}$;
- Avaliar o espectro de ação do complexo $[Fe(fen)_3]^{2+}$ frente a outras espécies bacterianas
- Obter o sistema lipídico nanoestruturado (SLN) e incorporar o complexo $[Fe(fen)_3]^{2+}$ ao mesmo;
- Caracterizar o sistema formado via dispersão de luz dinâmica e Potencial Zeta;
- Avaliar a morfologia do sistema formado utilizando Microscopia Eletrônica de Transmissão
- Avaliar a eficiência de encapsulação do sistema lipídico nanoestruturado;
- Avaliar o complexo incorporado ao sistema SLN+$[Fe(fen)_3]^{2+}$ frente a cepa H37Rv de *M. tuberculosis*

3. REFERÊNCIAS

ABOOFAZELI, R.; LAWRENCE, M. J. Investigations into the formation and characterization of phospholipid microemulsions. I. Pseudo-ternary phase diagrams of systems containing water-lecithin-alcohol-isopropyl myristate. **International Journal of Pharmaceutics**, v. 93, n. 1–3, p. 161–175, Maio 1993.

BARBERIS, I. et al. The history of tuberculosis: from the first historical records to the isolation of Koch's bacillus. **Journal of preventive medicine and hygiene**, v. 58, n. 1, p. E9–E12, Mar. 2017.

BAYDA, S. et al. The history of nanoscience and nanotechnology: From chemical-physical applications to nanomedicine. **Molecules**, v. 25, n. 1, p. 1–15, 2020.

BENCINI, A.; LIPPOLIS, V. 1,10-Phenanthroline: A versatile building block for the construction of ligands for various purposes. **Coordination Chemistry Reviews**, v. 254, n. 17–18, p. 2096–2180, Set. 2010.

BOTTEGA, F.C.; OLIVEIRA, M.R.L.; RUBINGER, M.M.M.; BELLATO, C.R.; ARDISSON, J.D.; ZAMBOLIM, L. Sais de tetrafenilfosfônio e *tris*(1,10-fenantrolina)ferro(II) de complexos aniônicos de dibutilenstanho(IV) com ditiocarbimatos: síntese, caracterização e atividade antifúngica. **Química Nova**. v. 39, n. 5, p. 554-560, 2016.

BHARTI, S. K.; SINGH, S. K. Metal Based Drugs : Current Use and Future Potential. **Der Pharmacia Lettre**, v. 1, p. 39–51, Jan. 2009.

CAMPOS, D. L. et al. Bactericidal effect of pyridine-2-thiol 1-oxide sodium salt and its complex with iron against resistant clinical isolates of Mycobacterium tuberculosis. **The Journal of Antibiotics**, v. 73, n. 2, p. 120–124, 2020.

CONSTANTINIDES, P. P. et al. Formulation and intestinal absorption enhancement evaluation of water-in-oil microemulsions incorporating medium-chain glycerides. **Pharmaceutical Research**, v. 11, n. 10, p. 1385–1390, Out. 1994.

COUTO, D. S. DE et al. Fatores determinantes para o abandono do tratamento da tuberculose: representações dos usuários de um hospital público. **Saúde em Debate**, v. 38, n. 102, p. 572–581, 2014.

CRISAN-DABIJA, R. et al. Tuberculosis and COVID-19 in 2020: lessons from the past viral outbreaks and possible future outcomes. **Canadian Respiratory Journal**, 1401053, Set. 2020.

DA SILVA, P. B. et al. In vitro activity of copper(II) complexes, loaded or unloaded into a nanostructured lipid system, against mycobacterium tuberculosis. **International Journal of Molecular Sciences**, v. 17, n. 5, 2016.

DA SILVA, P. B. et al. A nanostructured lipid system to improve the oral bioavailability of Ruthenium(II) complexes for the treatment of infections caused by Mycobacterium tuberculosis. **Frontiers in Microbiology**, v. 9, p. 1–11, Dez. 2018.

DE FREITAS, E. S. et al. Nanostructured lipid systems as a strategy to improve the in Vitro cytotoxicity of ruthenium(II) compounds. **Molecules**, v. 19, n. 5, p. 5999–6008, 2014.

DOS SANTOS FERNANDES, G. F. et al. Design, Synthesis, and Characterization of N-Oxide-Containing Heterocycles with in Vivo Sterilizing Antitubercular Activity. **Journal of Medicinal Chemistry**, v. 60, n. 20, p. 8647–8660, 2017.

FARIA-TISCHER, P. C. S.; TISCHER, C. A. Nanobiotecnologia: plataforma tecnológica para biomateriais e aplicação biológica de nanoestruturas. **Biochemistry and Biotechnology Reports**, v. 1, n. 1, p. 32–53, 20 Jun. 2012.

FEYNMAN, R. P. There's plenty of room at the bottom [data storage]. **Journal of Microelectromechanical Systems**, v. 1, n. 1, p. 60–66, 1992.

FONSECA-SANTOS, B.; GREMIÃO, M. P. D.; CHORILLI, M. Nanotechnology-based drug delivery systems for the treatment of Alzheimer's disease. **International journal of nanomedicine**, v. 10, p. 4981–5003, 2015.

GAO, E. et al. Synthesis, structures, molecular docking, cytotoxicity and bioimaging studies of two novel Zn(II) complexes. **European Journal of Medicinal Chemistry**, v. 121, p. 1–11, 2016.

GUPTA, S.; MOULIK, S. P. Biocompatible Microemulsions and Their Prospective Uses in Drug Delivery. **Journal of Pharmaceutical Sciences**, v. 97, n. 1, p. 22–45, Jan. 2008.

HOMAYUN, B.; LIN, X.; CHOI, H.-J. Challenges and Recent Progress in Oral Drug Delivery Systems for Biopharmaceuticals. **Pharmaceutics**, v. 11, n. 3, p. 129, 19 Mar. 2019.

HOTTINGER, D. G. et al. Sodium nitroprusside in 2014: A clinical concepts review. **Journal of Anaesthesiology, Clinical Pharmacology**, v. 30, n. 4, p. 462–471, Out. 2014.

IDRISS, K. A. et al. Spectral properties and analytical application of the ternary complex of lanthanum(III) with 1,10-phenanthroline and eosin. **Analytica Chimica Acta**, v. 116, n. 2, p. 413–416, 1980.

KHAN, I. et al. Nanobiotechnology and its applications in drug delivery system: a review. **IET Nanobiotechnology**, v. 9, n. 6, p. 396–400, Dec. 2015.

KOCH, S.; ACKERMANN, G. Application of redox reactions in spectrophotometry—I The iron(III)/1,10-phenanthroline complex as a reagent for the determination of some anions and organic compounds. **Talanta**, v. 39, n. 6, p. 687–691, 1992.

LORENZO, E. et al. Analytical strategies for amperometric biosensors based on chemically modified electrodes. **Biosensors and Bioelectronics**, v. 13, n. 3, p. 319–332, 1998.

MAHAJAN, R. Bedaquiline: First FDA-approved tuberculosis drug in 40 years. **International Journal of Applied & Basic Medical Research**, v. 3, n. 1, p. 1–2, Jan. 2013.

MAINARDES, R. M. et al. Liposomes and Micro/Nanoparticles as Colloidal Carriers for Nasal Drug Delivery. **Current Drug Delivery**, 2006.

MCCANN, M. et al. Synthesis and X-ray crystal structure of [Ag(phendio)2]ClO_4

(phendio = 1,10-phenanthroline-5,6-dione) and its effects on fungal and mammalian cells. **BioMetals**, v. 17, n. 6, p. 635–645, Nov. 2004.

MINISTÉRIO DA SAÚDE BRASIL. **Brasil Livre da Tuberculose: Plano Nacional pelo Fim da Tuberculose como Problema de Saúde Pública,** 2017.

NASIRUDDIN, M.; NEYAZ, M. K.; DAS, S. Nanotechnology-Based Approach in Tuberculosis Treatment. **Tuberculosis Research and Treatment**, 4920209, 2017.

OCHEKPE, N. A.; OLORUNFEMI, P. O.; NGWULUKA, N. C. Nanotechnology and drug delivery part 1: Background and applications. **Tropical Journal of Pharmaceutical Research**, v. 8, n. 3, p. 265–274, 2009.

PAI, M. et al. Tuberculosis. **Nature Reviews Disease Primers**, v. 2, 2016.

PAVAN, F. R. et al. Thiosemicarbazones, semicarbazones, dithiocarbazates and hydrazide/hydrazones: anti-Mycobacterium tuberculosis activity and cytotoxicity. **European journal of medicinal chemistry**, v. 45, n. 5, p. 1898–1905, May 2010.

PAVAN, F. R. et al. Ruthenium(II) phosphine/diimine/picolinate complexes: Inorganic compounds as agents against tuberculosis. **European Journal of Medicinal Chemistry**, v. 46, n. 10, p. 5099–5107, 2011.

PENTENERO, M. Nanotechnology: a novel adjunctive aid to fight cancer. **Oral Diseases**, v. 23, n. 3, p. 273–275, Apr. 2017.

RABAHI, M. F. et al. Tratamento da tuberculose. **Jornal Brasileiro de Pneumologia**, v. 43, n. 5, p. 472–486, 2017.

RUSSELL, D. G. Who puts the tubercle in tuberculosis? **Nature reviews. Microbiology**, v. 5, n. 1, p. 39–47, Jan. 2007.

RYAN, N. J.; LO, J. H. Delamanid: First Global Approval. **Drugs**, v. 74, n. 9, p. 1041–1045, 2014.

SAFARI, J.; ZARNEGAR, Z. Advanced drug delivery systems: Nanotechnology of health design A review. **Journal of Saudi Chemical Society**, v. 18, n. 2, p. 85–99, Apr. 2014.

SHETYE, G. S.; FRANZBLAU, S. G.; CHO, S. New tuberculosis drug targets, their inhibitors, and potential therapeutic impact. **Translational Research**, v. 220, p. 68–97, 2020.

SILVA, D. R. et al. Tuberculosis and COVID-19, the new cursed duet: What differs between Brazil and Europe? **Jornal Brasileiro de Pneumologia**, v. 47, n. 2, p. 1–8, 2021.

SILVA, P. DA F. et al. Fatores associados ao abandono do tratamento da tuberculose pulmonar no Maranhão, Brasil, no período de 2001 a 2010. **Cadernos de Saúde Pública**, v. 30, n. 8, p. 1745–1754, 2014.

SOLCIA, M. C. et al. Growth-inhibitory effects of tris-(1,10-phenanthroline) iron (II) against Mycobacterium tuberculosis in vitro and in vivo. **Tuberculosis**, v. 128, n. April, p. 1–8, 2021.

TARALLO, M. B. et al. Design of novel iron compounds as potential therapeutic agents against tuberculosis. **Journal of Inorganic Biochemistry**, v. 104, n. 11, p. 1164–1170, 2010.

TENJARLA, S. Microemulsions: an overview and pharmaceutical applications. **Critical Reviews in Therapeutic Drug Carrier Systems**, v. 16, n. 5, p. 461–521, 1999.

UÇAR, I. et al. Tris(1,10-phenanthroline-k2N,N′)iron(II) squarate octahydrate. **Acta Crystallographica Section E: Structure Reports Online**, v. 61, n. 7, p. 1405–1407, 2005.

VAN DER MEEREN, O. et al. Phase 2b Controlled Trial of M72/AS01E Vaccine to Prevent Tuberculosis. **New England Journal of Medicine**, v. 379, n. 17, p. 1621–1634, 25 Set. 2018.

VASAVA, M. S. et al. Drug development against tuberculosis: Past, present and future. **Indian Journal of Tuberculosis**, v. 64, n. 4, p. 252–275, 2017.

VISCA, D. et al. Tuberculosis and COVID-19 interaction: A review of biological, clinical and public health effects. **Pulmonology**, v. 27, n. 2, p. 151–165, 2021.

WADA, O. What are Trace Elements ? — Their deficiency and excess states. **Japan Medical Association Journal**, v. 47, n. 5, p. 351, 2004.

WARD, S. K.; HOYE, E. A.; TALAAT, A. M. The global responses of Mycobacterium tuberculosis to physiological levels of copper. **Journal of Bacteriology**, v. 190, n. 8, p. 2939–2946, 2008.

WEISSIG, V.; PETTINGER, T. K.; MURDOCK, N. Nanopharmaceuticals (part 1): products on the market. **International journal of nanomedicine**, v. 9, p. 4357–4373, 2014.

WELLINGTON, S.; HUNG, D. T. The Expanding Diversity of Mycobacterium tuberculosis Drug Targets. **ACS Infectious Diseases**, v. 4, n. 5, p. 696–714, 11 Maio 2018.

WORLD HEALTH ORGANIZATION (WHO). **Global Tuberculosis ReportWorld Health Organization**. [s.l: s.n.].

WORLD HEALTH ORGANIZATION (WHO). **The Paradigm Shift - Global Plan to End TBWorld Health Organization**. [s.l: s.n.].

WORLD HEALTH ORGANIZATION, (WHO). **WHO report on TB 2020**. [s.l: s.n.]. v. 1

WORLD HEALTH ORGANIZATION, (WHO). **WHO report on TB 2020**. [s.l: s.n.]. v. 1

WORLD HEALTH ORGANIZATION (WHO). **Meeting report of the WHO expert consultation on the definition of extensively drug-resistant tuberculosis**. [s.l: s.n.].

YANG, H.; LU, S. COVID-19 and tuberculosis. **Journal of Translational Internal Medicine**, v. 8, n. 2, p. 59–65, 2020.

ZHANG, Y.; SEN, S.; GIEDROC, D. Iron Acquisition by Bacterial Pathogens: Beyond tris-Catecholate Complexes. **ChemBioChem**, Mar. 2020.

ZUMLA, A.; NAHID, P.; COLE, S. T. Advances in the development of new tuberculosis drugs and treatment regimens. **Nature Reviews Drug Discovery**, v. 12, p. 388, 2013.

Capítulo II

tris1,10-phenantroline iron (II) loaded into a nanostructured lipid system: characterization and anti-*tuberculosis* activity

Rachel Temperani Amaral Machado[1], Camila Maringolo Ribeiro[1], Maria Carolina Franzini[1], Melina Borges Teixeira[2], Amauri A. Menegário[2], Marcia Cristina Oliveira da Rocha[3], Sônia Nair Báo[3], Patrícia Bento da Silva[4], Fernando Rogério Pavan[1*].

[1]Tuberculosis Research Laboratory, School of Pharmaceutical Sciences, Biological Sciences Department, São Paulo State University (UNESP), Araraquara, São Paulo, Brasil;

[2]Environmental Studies Center, São Paulo State University (UNESP), Rio Claro, 13506-13 900 São Paulo, Brazil;

[3] Electron Microscopy Laboratory, Cell Biology Department, Institute of Biological Sciences, University of Brasilia, Brasília, 70910,900, Brazil;

[4] Laboratory of Nanobiotechnology, Department of Genetics and Morphology, Institute of Biological Sciences, University of Brasilia, Brasilia, 70910-900, Brazil

***** Corresponding Author: *Department of Biological Sciences, School of Pharmaceutical Sciences, Rodovia Araraquara-Jaú, Km 01, Campos Ville, CEP 14800-903, Araraquara-SP, Brazil. Phone number +55 16 33014671. Email address: fernando.pavan@unesp.br*

Abstract

Tuberculosis (TB) causes approximately 10 million cases per year worldwide. In addition, the high rates of resistance to the main classes of antimicrobials contribute to TB being among the greatest causes of death from an infectious agent. Thus, the need to control and combat this disease, which represents a serious threat to global public health, is evident. Therefore, it is necessary to face the challenge of developing new active agents against TB. Previous studies showed the complex ($[Fe(phen)_3]^{2+}$) to be a possible anti-TB candidate. In this work, we present a synthesis and characterization of a nanostructured lipid system (NLS) that can deliver and protect the complex, and we report further biological activities of the complex. The frequency of *Mycobacterium tuberculosis* resistance to $[Fe(phen)_3]^{2+}$ is lower than that of other first-line drugs for treating tuberculosis, such as rifampicin. It presented a MIC_{90} value of 4.17 µM on its free form and 23.39 µM when loaded into the NLS. The complex has a narrow spectrum of action and does not act against intestinal microbiota bacteria. The NLS+$[Fe(phen)_3]^{2+}$ formulation was stable for up to 90 days at 5 ºC and after dilution in various media. The NLS showed an entrapment efficiency rate close to 60% of $[Fe(phen)_3]^{2+}$. Particles of NLS+$[Fe(phen)_3]^{2+}$ were homogeneous (PdI = 0.17), with a negative surface charge of -34.7 mV and an average size of 163 nm, defined by the dynamic light scattering (DLS) technique and confirmed by transmission electron microscopy (TEM), which also revealed their spherical morphology. These findings suggest that $[Fe(phen)_3]^{2+}$ is a potential novel therapeutic for TB and, when loaded into the NLS, it could be administered by the oral route.

Keywords: *Mycobacterium tuberculosis*$_1$, Phenantroline$_2$, *tris1,10-phenantroline iron (II)*$_3$, Nanostructured lipid system$_4$, new antmicrobials$_5$.

Introduction

Despite its ancient origins, tuberculosis (TB) still represents a major challenge for public health worldwide. TB is an infectious disease, in which *Mycobacterium tuberculosis* is the main etiological agent species. The World Health Organization (WHO) estimated about 10 million cases of TB and 1.4 million deaths as a result of the disease, globally in 2019 (World Health Organization 2020a).

The current standard TB treatment regimen, for non-resistant strains, is based on four drugs, rifampicin (RIF), isoniazid (INH), ethambutol (ETB), and pyrazinamide (PZA) which were developed in the 20th century (Ministério da Saúde Brasil 2017). After several decades without new drugs for the TB treatment, the drugs bedaquiline, delamanid, pretomanid and linezolid have been approved for use in clinical practice (World Health Organization 2020a). And even for these newly developed drugs there are already reports of mycobacterial resistance (Rabahi et al. 2017; Ignatius and Dooley 2019).

Multidrug resistant TB (MDR-TB) is defined as resistance of the bacillus to the two main first-line drugs, INH and RIF. A new definition from the World Health Organization is the extended pre-resistance form (Pre-TB-XDR), which is characterized by resistance to INH and RIF plus any of the fluoroquinolones. The extended resistance form (TB-XDR) meets the definition of Pre-TB-XDR and is also resistant to one of the second-line drugs, levofloxacin, moxifloxacin, bedaquiline and linezolid (World Health Organization (WHO) 2021).

A major problem faced to combat TB is the high resistance of the bacteria to the existing drugs. The pathogen continues to evolve and develop complex resistance patterns to the drugs available in therapy. The fact that approximately 17% of people do not complete the drug therapy, further contributes to the increase in bacterial resistance (Couto et al. 2014; P. da F. Silva et al. 2014).

Considering these facts, the need to develop newer, more potent, and safer anti-TB drugs, with a novel mechanism of action, and able to eliminate drug-resistant bacilli overcoming the traditional resistance mechanisms and optimizing the TB treatment, becomes evident (Vasava et al. 2017; Wellington and Hung 2018).

Toward the last decades, especially after the discovery of cisplatin, inorganic chemistry reached great prominence in its contribution to medicine, and to this day is gaining importance through the knowledge acquired about the central importance of

inorganic elements in organisms (Orvig and Abrams 1999). Phenanthroline (phen) is a highly versatile chemical ligand, it has various therapeutic applications through the formation of complexes with different transition metals (Gao et al. 2016). Metal ions, including iron, can exhibit a wide range of antimicrobial activity, mainly as iron oxide nanoparticles (de Toledo, Rosseto, and Bruschi 2018).

Tris-(1,10-phenanthroline) iron (II) ($[Fe(phen)_3]^{2+}$), is formed by the complexation of the phen ligand and iron. The work conducted by Solcia *et al.* demonstrated the metal complex ($[Fe(phen)_3]^{2+}$) had an excellent activity against *M. tuberculosis*, including the sensible laboratorial strains H37Rv and resistant clinical isolates in normal and modified conditions and also antimycobacterial intracellular activity comparable to RIF, *in vitro*. Furthermore, when ($[Fe(phen)_3]^{2+}$) was loaded into a nanostructured lipid system (NLS) it became oral bioavailable in BALB/c mice showing a maximum concentration within 6h (Solcia et al. 2021).

Oral delivery has been recognized as the most convenient and attractive method to deliver drugs, mostly because of its ease of administration. However, this route is full of challenges due to the presence of variety of active enzymes in the gastrointestinal tract, the low permeability of the intestinal epithelium and the hepatic barriers after the entry through the vessels under the intestinal epithelium led to a lower bioavailability of some orally administered drugs (Homayun, Lin, and Choi 2019). One strategy widely used to bypass these challenges is to protect them by loading into a biocompatible and biodegradable nanoparticles system (des Rieux et al. 2007).

Nanotechnology-based drug delivery systems have shown great results in the treatment of infectious diseases, including TB. Different types of nanocarriers are promising drug delivery systems for various routes of administration, covering oral and inhalation administration. These systems have high stability, improved bioavailability of the drug, can also reduce dosing frequency and solve the difficulty of low compliance, a major obstacle in the controlling of TB epidemic (P. B. da Silva et al. 2016; P. B. Da Silva et al. 2018; E. S. De Freitas et al. 2014; Dos Santos Fernandes et al. 2017; Nasiruddin, Neyaz, and Das 2017).

From the promising results mentioned above, the need for more detailed studies on the activity of ($[Fe(phen)_3]^{2+}$) and on the system formed with its incorporation into the NLS arose. In this work we aimed at the evaluation of the ($[Fe(phen)_3]^{2+}$) activity against different bacterial genera, mutation frequencies against *M. tuberculosis*

sensible H37Rv strain, its incorporation into a NLS, characterization of the obtained formulation and determination of its stability.

Materials and Methods

1. Compounds and anti-TB drugs

The $[Fe(phen)_3]^{2+}$ aqueous solution (692.52 M; $[Fe(C_{12}H_8N_2)_3]SO_4$) was purchased from Sigma-Aldrich®. The stock solutions of RIF and INH (10 mg/mL) were prepared in dimethylsulfoxide (DMSO) - Sigma-Aldrich®) and stored at -20ºC.

2. Bacterial culture

The bacterial culture was kept frozen in cryotubes with 20% glycerol at -80°C. The *M. tuberculosis* H37Rv strain (ATCC 27294) was cultured in Middlebrook 7H9 broth (Sigma-Aldrich®) supplemented with 10% oleic acid, albumin, dextrose and catalase (OADC), at 120rpm and 37ºC until the turbidity of the culture reached the McFarland standard of 1.0.

3. Fourier Transform Infrared (FTIR)

$[Fe(phen)_3]^{2+}$ solution and the same one after a freeze-drying process were mixed in KBr for Merck spectroscopy and pressed in a wafer for 1 min, 10-ton pressure. The analyses were performed in Thermo Scientific NICOLET IS5 equipment, iD3 module with attenuated total reflectance (ATR), spectral resolution of $2cm^{-1}$, 32 scans in the range 4000-400 cm^{-1}

4. Biological Assays

a. Evaluation of activity spectrum

The antibacterial activity of $[Fe(phen)_3]^{2+}$ against bacteria other than *M. tuberculosis* was evaluated using broth microdilution assays, in order to determine the substance spectrum. We evaluated Gram-positive and Gram-negative bacteria, including ESKAPE pathogens and microbiota bacteria (Table 2). The assays were performed according to the European Committee on Antimicrobial Susceptibility Testing (EUCAST).

b. **Resistance frequencies**

7H11 agar plates were prepared containing increasing concentrations of $[Fe(phen)_3]^{2+}$, 1x, 2x, 4x, 6x, and 8x the MIC_{99} value on solid medium, 1.56 µg/mL (2.62 µM) and supplemented with 10% OADC to determine the resistance frequency. From a culture of *M. tuberculosis* ($1.12x10^{12}$ CFU/mL), 100uL were seeded onto each 7H11 agar plate containing the different concentrations of $[Fe(phen)_3]^{2+}$ and incubated at 37°C for 4 weeks.

c. **Anti-Mycobacterium tuberculosis analysis**

To determine minimal inhibitory concentration (MIC_{90}) of $[Fe(phen)_3]^{2+}$ incorporated into the NLS against standard strain of *Mycobacterium tuberculosis* H_{37}Rv the Resazurin Microtiter Assay (REMA) was used (Palomino et al. 2002). The samples, diluted in a range concentration of 0.09 to 25 mg/mL, were added to a 96-well microplate with the bacterial inoculum (10^5 CFU ml^{-1}). The plates were incubated for 7 days at 37 ºC, 5,0% CO_2 atmosphere. Next, resazurin 0.01% was added and after incubation of 24h, the fluorescence was read at 530/590 nm. Two replicates were performed. The MIC_{90} was defined as the lowest concentration of compound able to inhibit 90% of mycobacterial growth.

5. **NLS obtaining and $[Fe(phen)_3]^{2+}$ incorporation**

The NLS is composed by 10% oil phase (cholesterol), 10% surfactant (a mixture of soy phosphatidylcholine, sodium oleate and Eumulgin® HRE 40 [hydrogenated polyoxyl castor oil 40]; 3: 6: 8) and 80% aqueous phase (saline-phosphate buffer [PBS] pH 7.4). The mixture was sonicated using a rod sonicator (Q700 from QSonica®, Newtown, CT, USA), 700 watts, in discontinuous mode for 10 minutes with a 30 second interval every minute, with ice bath during the process. Afterwards, the obtained NLS was centrifuged at 11,180 × g for 15 minutes to eliminate particles released from the titanium rod. $[Fe(phen)_3]^{2+}$ was first freeze-dried, and then loaded into a NLS (NLS+$[Fe(phen)_3]^{2+}$) at the concentration of 3000 µg/mL by sonication for 3 minutes (E. S. De Freitas et al. 2014).

6. NLS Characterization

a. Microscopy

The size and morphology of nanoparticles were characterized using a transmission electron microscope (TEM; JEOL 1011, Tokyo, Japan) operated at an accelerating voltage of 100 kV. Samples were prepared by placing a drop of sample (5 µL) using a 400-mesh copper grid coated with formvar film, and then it was air-dried, following contrast enhancement with osmium tetroxide vapor. Grids were kept at room temperature until analysis.

b. Dynamic Light Scattering (DLS)

The determination of the mean particle size (Z average) and the polydispersity index (PdI) was performed by the photon correlation technique, developed by Silva *et al.*, known as quasi-elastic light scattering (J. A. da Silva et al. 2009). The zeta potential (ZP) analysis was performed by determining the electrophoretic mobility of the lipid system. The samples were diluted at a ratio of 1:10 (w/v) in distilled water, and the parameters were analyzed using DLS equipment (Zetasizer Nano NS, Malvern Instruments, Malvern, UK).

c. Storage Stability

The storage stability of the formulations was performed for up to 90 days under three different temperatures, at 37 ± 0.5 °C, room temperature (25 ± 4°C) and 5 ± 1 °C as described by Araujo et al. (Araujo et al. 2020). The parameters considered to evaluate stability were Z average, PdI and ZP using a DLS equipment (Zetasizer Nano NS, Malvern Instruments, Malvern, UK). Three determinations of ZP and ten determinations of Z Average and PdI of the droplets were performed, calculating mean and standard deviation. Statistical significance was considered when $p<0.05$, with a 95% confidence interval.

d. Stability in culture media and solutions with different pHs

Z average, PdI and ZP were evaluated 24 hours after dilution of the formulations, which contained or not the incorporated complex $[Fe(phen)_3]^{2+}$, in solutions of 0.1M HCl at pH 1.0 and phosphate buffer at pH 7.4, corresponding to stomach and blood pH respectively (Freire et al. 2006), in order to estimate the stability of the formulations

under these conditions. The formulations were also evaluated in the presence of culture media used for the cultivation of *M. tuberculosis*, 7H9, and for the cultivation of eukaryotic cells Dulbecco's Modified Eagle's Medium (DMEM) with high glucose concentration (Da Rocha et al. 2020). Statistical significance was considered when $p<0.05$, by the Two-way ANOVA test.

e. **Entrapment efficiency and Drug loading capacity**

The evaluation of the entrapment efficiency (EE%) and drug loading capacity (DL%) of $[Fe(phen)_3]^{2+}$ was performed using the ultracentrifugation method, with some adjustments, as performed by Laouini et al. (Laouini et al. 2013). The volume of 0.5 mL of NLS+$[Fe(phen)_3]^{2+}$ was centrifuged in a 5417R centrifugue (Eppendorf AG) at 14000 rpm at 4°C for 30 minutes. Then, 250 µL of the supernatant was added to 250 µL of a Triton™X-100 0.1% solution to promote separation of $[Fe(phen)_3]^{2+}$ from the others lipid components. The same dilution was performed for the sample of NLS+$[Fe(phen)_3]^{2+}$ that did not undergo centrifugation. The samples were then subjected to 15 minutes ultrasonic bath, and then centrifuged at 4000 rpm for 5 minutes, for the sedimentation of residual lipids.

Total iron content was determined by Inductively Coupled Plasma Mass Spectrometrometry (ICP-MS), as described in the following. Two independent assays were performed in two distinct NLS+$[Fe(phen)_3]^{2+}$ formulations, obtained separately. EE% and DL% were calculated using equations 1 and 2, respectively.

$$EE\% = \frac{Ecapsulated\ amount\ of\ drug}{total\ amount\ of\ drug} x100 \qquad (1)$$

$$DL\% = \frac{Encapsulated\ amount\ of\ drug}{lipid\ content} x100 \qquad (2)$$

f. **Quantification by Inductively Coupled Plasma Mass Spectrometrometry (ICP-MS)**

The concentration of Fe was determined using an Inductively Coupled Plasma Mass Spectrometry (ICP-MS, iCAP RQ, Thermo Scientific, Germany) at *m/z* 56 ($^{56}Fe^{+}$). In order to remove polyatomic spectral interferences, the detection mode kinetic energy discrimination was used. The analytical curve for Fe was from 0.0 to 500 µg L^{-}

[1] using a multielemental stock solution (100 mg L^{-1}). All standards and samples were prepared in HNO_3 2 % (v/v). A certified reference material EnviroMAT Wastewater, Low (EU-L) (SPC Science, Canada) was also analyzed to ensure the quality of the measurements. As an internal standard, a 100 µg/L solution of ^{45}Sc and ^{89}Y was used during analyses. The limit of detection (LOD) for iron was 1.3 µg/L.

Results

1. Fourier Transform Infrared (FTIR)

The vibrational spectra in the infrared region of the aqueous solution of $[Fe(phen)_3]^{2+}$ and of it after freeze-drying, a process that was necessary for the incorporation of it into the lipid system, was performed in order to observe possible changes in the vibrational properties of the molecule after the water removal process. These changes are observed through the disappearance, appearance, enhancement, or displacement of the vibrational modes of the molecule shown in the spectra presented in Figure 1 and Table 1.

When comparing the two spectra of $[Fe(phen)_3]^{2+}$ from the solution and the freeze-dried sample, it can be seen that the peaks present in the freeze-dried sample are better defined, probably due to the absence of the water that was removed in the process. However, the peak that is assigned to the vOH referring to the aqueous solution (presence of water) in the sample at 3452 cm^{-1}, is still observed at 3414 cm^{-1} in the freeze-dried sample, indicating the presence of moisture in this last one. The stretching vibration peaks of the vC=N and vC=C double bonds are observed at 1640 and 1637 cm^{-1}, and at 1628 and 1618 cm^{-1} for aqueous solution and freeze-dried $[Fe(phen)_3]^{2+}$, respectively (Wang et al. 2015).

The peak at 1105 cm^{-1} and at 1099 cm^{-1} for aqueous solution and freeze-dried $[Fe(phen)_3]^{2+}$, respectively, is attributed to vCC + δCH. At 727 cm^{-1} a defined peak of medium intensity is observed referring to the out-of-plane deformation vibration of the C-H bond of phenanthroline (phen), however, in this region a broadened band is observed for the aqueous solution sample probably attributed to the presence of water, which makes it difficult to identify this same peak attributed to γCH (Gerasimova and Katsyuba 2013).

By analyzing the aqueous solution and the freeze-dried samples of $[Fe(phen)_3]^{2+}$ in the infrared, and making a comparison of the spectra, it can be stated that the coordination compound is the same and that the freeze-drying process didn´t destructure the sample.

Table 1. Vibrational frequencies in the infrared region (cm^{-1}) referring to the aqueous solution and freeze-dried $[Fe(phen)_3]^{2+}$, and their respective assignments

Samples		Assignments
$[Fe(phen)_3]^{2+}$ Aqueous solution	**($[Fe(fen)_3]^{2+}$) Freeze-dried**	
3452	3414	νO-H
2924	2927	νC-H
1640	1640	νC=N
1628	1620	νC=C
1105	1099	νCC + δCH
-	727	γCH

Figure 1.Vibrational spectra in the infrared region of the aqueous solution and freeze-dried $[Fe(phen)_3]^{2+}$

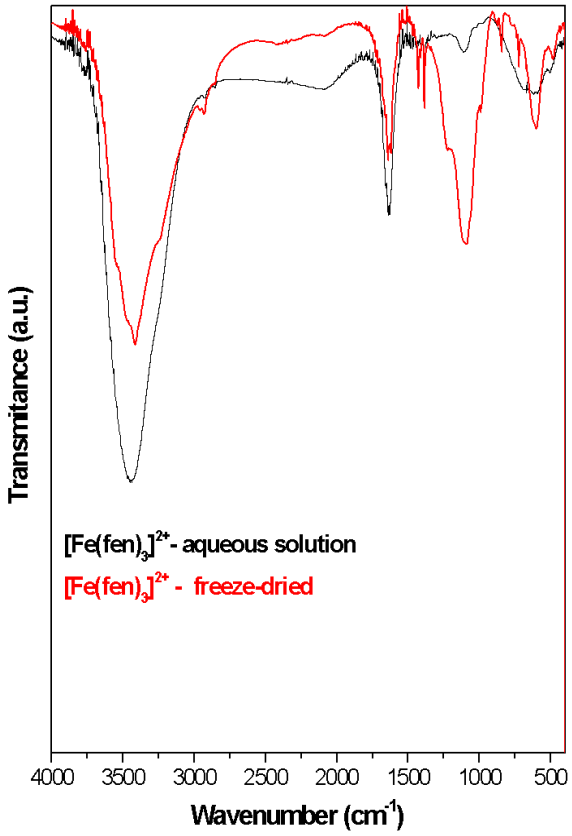

2. **Biological Assays**

a. **Evaluation of activity spectrum**

$Fe(phen)_3]^{2+}$ did not show a MIC_{90} value (it was not antibacterial) up to a concentration of 100 ug/mL, against any of the strains evaluated, demonstrating a similar profile to the first-line drug, INH, which also did not show a MIC_{90} value up to the same concentration. $[Fe(phen)_3]^{2+}$ can be classified as a molecule with a narrow spectrum activity, specific in inhibiting mycobacteria, in view of its demonstrated activity against *M. tuberculosis* and *M. smegmatis* (Solcia et al. 2021).

Table 2. Minimum inhibitory concentration (MIC_{90}) of $[Fe(phen)_3]^{2+}$, rifampicin (RIF) and isoniazid (INH) against a variety of bacterial strains.

Strain	MIC $_{90}$(µg/mL)		
	$[Fe(phen)_3]^{2+}$	RIF	INH
Staphylococcus saprophyticus (ATCC 15305)	>100	0,007	>100
Staphylococcus epidermidis (ATCC 14990T)	>100	0,001	>100
Klebsiella pneumoniae (ATCC 13883T)	>100	4	>100
Klebsiella oxytoca (CCT-0182)	>100	6,3	>100
Enterobacter cloacae (ATCC 13883T)	>100	128	>100
Enterobacter aerogenes (ATCC 13048T)	>100	128	>100
Enterococcus faecium (NCTC 7171T)	>100	0,3	>100
Enterococcus faecalis (ATCC 29212)	>100	0,003	>100
Proteus mirabilis (ATCC 29906T)	>100	16	>100
Citrobacter freundii (ATCC 8090T)	>100	32	>100

b. **Resistance frequencies**

Growth of a "mat" of cells was observed on the two plates containing 1 x MIC_{99} of the $[Fe(fen)_3]^{2+}$ and absence of growth on the plates with higher concentrations of the complex. With this result, it can be inferred that, at a concentration equal to or higher

than 2x the MIC_{99}, i.e 3.12 µg/mL or 5.23 µM, the complex presents a resistance frequency lower than 10^{-12}, expressing a low probability of finding one resistant bacillus to the complex, which is ideal for therapy. Moreover, it presents a lower resistance frequency rate than that found for first-line TB treatment drugs, such as RIF, which is around 10^{-9} at a concentration of 2 µg/mL or 2.43 µM (Ford et al. 2011), equivalent to approximately 4 times the MIC_{99} value of this drug (Lee and Heifets 1987).

c. **Anti-Mycobacterium tuberculosis analysis**

The inhibitory activity of NLS+$[Fe(phen)3]^{2+}$ against *M. tuberculosis* was investigated in this assay and the results are shown in Table 3. The complex was shown to be active both in its free form and load into the NLS with MICs of 4.17 and 23.39 µM, respectively. The MIC_{90} of $[Fe(phen)3]^{2+}$ was extensively covered in the work carried out by Solcia *et al.* (2021) and it was similar to what was found here.

Table 3. Determination of minimum inhibitory concentration (MIC_{90}) of tris-(1,10-phenanthroline) iron (II) complex against the sensitive strain Mycobacterium tuberculosis H37Rv.

Samples	MIC_{90}	
	(µg/mL ± sd)	(µM ± sd)
$[Fe(phen)_3]^{2+}$	2.48 ± 0.41	4.17 ± 0.41
NLS+$[Fe(phen)_3]^{2+}$	13.94 ± 1.52	23.39 ± 1.52
RIF	0.11 ± 0.004	0.13 ± 0.004

$[Fe(phen)_3]^{2+}$ = tris-(1,10-phenanthroline) iron (II); NLS+$[Fe(phen)_3]^{2+}$ = tris-(1,10-phenanthroline) iron (II) loaded into the nanostructured lipid system; RIF = rifampicin; Values are the average of two experiments.

3. **NLS and NLS+[Fe(phen)$_3$]$^{2+}$ Characterization**

a. **DLS data and TEM images**

Incorporation of the [Fe(phen)$_3$]$^{2+}$ complex into the NLS resulted in a slight right shift of the intensity curve, observed in the DLS data in figure 2 (I), implying an increase in average particle size, from 140.5 nm to 163 nm. The negative charge surface of the NLS particles undergoes a faint decrease in modulus, when coupled with NLS+[Fe(phen)$_3$]$^{2+}$, as inferred from the ZP results in Figure 2 (II). The morphology of NLS and NLS+[Fe(phen)$_3$]$^{2+}$ nanoparticles were characterized by TEM, on figure 2 (III). Both particles reveal a spherical shape and have size uniformity. The diameters of the NLS and NLS+[Fe(phen)$_3$]$^{2+}$ nanoparticles were compatible with particle size results from DLS technique.

Figure 2.(I) DLS size distribution by intensity for NLS and NLS+[Fe(phen)$_3$]$^{2+}$; (II) Zeta Potential for NLS and NLS+[Fe(phen)$_3$]$^{2+}$. (III) TEM micrographs illustrating the size and morphology: (A) NLS, 5K Magnification; (B)NLS, 10k Magnification; (C) NLS+[Fe(phen)$_3$]$^{2+}$, 5K Magnification and (D) NLS+[Fe(phen)$_3$]$^{2+}$, 10k Magnification.

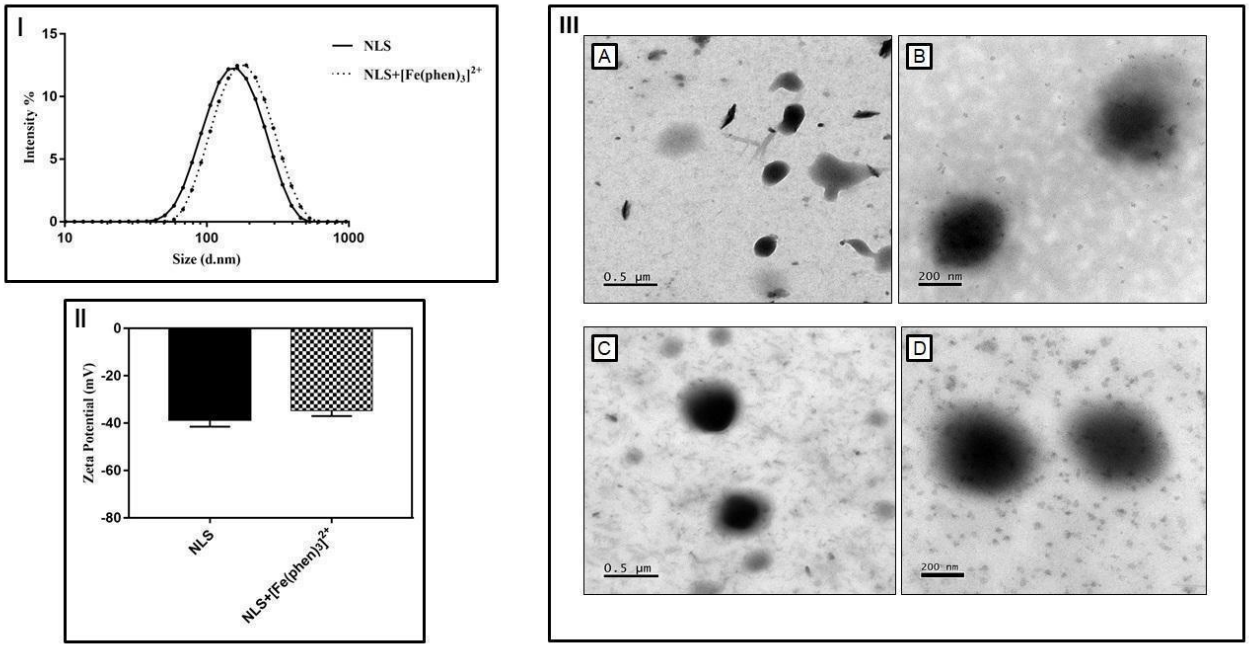

b. **Storage Stability**

NLS and NLS+[Fe(phen)$_3$]$^{2+}$ stored in 5ºC didn´t display significant changes in Z Average, for 90 days, when compared to the 1st day of analysis, where the mean and standard deviation for NLS was 145.53 ± 0.90 nm, and for NLS+[Fe(phen)$_3$]$^{2+}$ was 156.90 ± 4.49 nm. The same was shown for PdI that remained stable, 0.15 ± 0.01 in

both cases. The ZP values in 5ºC showed no significant changes in 90 days, varying from -38.33 ± 2.18 to -44.00 ± 2.78 mV for NLS and from -33.80 ± 1.47 to -37.60 ± 1.61 mV for NLS+$[Fe(phen)_3]^{2+}$ (Figure 3).

At room temperature, the NLS didn´t undergo significant changes of Z Average and PdI until the 60th day of analysis, but on the 90th day it showed an increase of Z Average going from 144.90 ± 1.00 nm to 184.40 ± 3.57 nm and PdI going from 0.17 ± 0.02 to 0.45 ± 0.03. NLS+$[Fe(phen)_3]^{2+}$ showed a significant increase in values earlier, on the 60th day, changing from 162.97 ± 0.35 nm and 0.16 ± 0.02 to 177.43 ± 4.47 nm and 0.38 ± 0.03, Z Average and PdI, respectively. ZP showed variation from -38.57 ± 2.82 to -43.00 ± 1.64 mV in the case of NLS and -34.70 ± 2.26 to -46.10 ± 1.51 mV for the NLS+$[Fe(phen)_3]^{2+}$ (Figure 4).

At 37ºC NLS remained without significant changes ($p<0.05$) until the 30th day of analysis for the Z Average and PdI parameters, but on the 60th day it shows a slight increase in the two parameters presented, ranging from 143.70 ± 4.91 nm and 0.15 ± 0.03 to 153.80 ± 1.29 nm and 0.24 ± 0.01. However, NLS+$[Fe(phen)_3]^{2+}$ showed a significant increase ($p<0.05$) from 30th day of analysis, going from 162.40 ± 1.83nm and 0.17 ± 0.02 on the first day of analysis to 236.30 ± 5.82 nm and 0.50 ± 0.04 on the last day, Z Average and PdI values, respectively. The ZP of both formulations showed significant ($p<0.05$) decrease on the 60th day ranging from -41.30 ± 2.00 to -46.30 ± 1.85 mV for NLS and from -34.00 ± 2.00 to -48.63 ± 3.45 mV for NLS+$[Fe(phen)_3]^{2+}$ (figure 5).

The NLS+$[Fe(phen)_3]^{2+}$ formulations conditioned at room temperature and at 37ºC were not analyzed on the 90th day, due to the formation of a film caused by water evaporation through capillary forces resulting from dehydration, a circumstance also observed by Müller, Radtke, and Wissing (Müller, Radtke, and Wissing 2002). The increase in Z Average and PdI values and the decrease in ZP values are a strong indication of aggregate formation by particle coalescence, which can be observed gradually with the increasing temperature. Despite these modifications mentioned above, the values for both formulations especially when stored at 5ºC demonstrate great uniformity and stability up to 90 days of analysis.

Figure 3. Values and 95% confidence interval of the Average particle size (Z Average), Zeta potential (ZP) and the polydispersity index (PdI), of the NLS and NLS+$[Fe(phen)_3]^{2+}$ formulations, over 90 days stored at 5ºC. Three determinations of ZP and ten determinations of Z Average and PdI were performed.

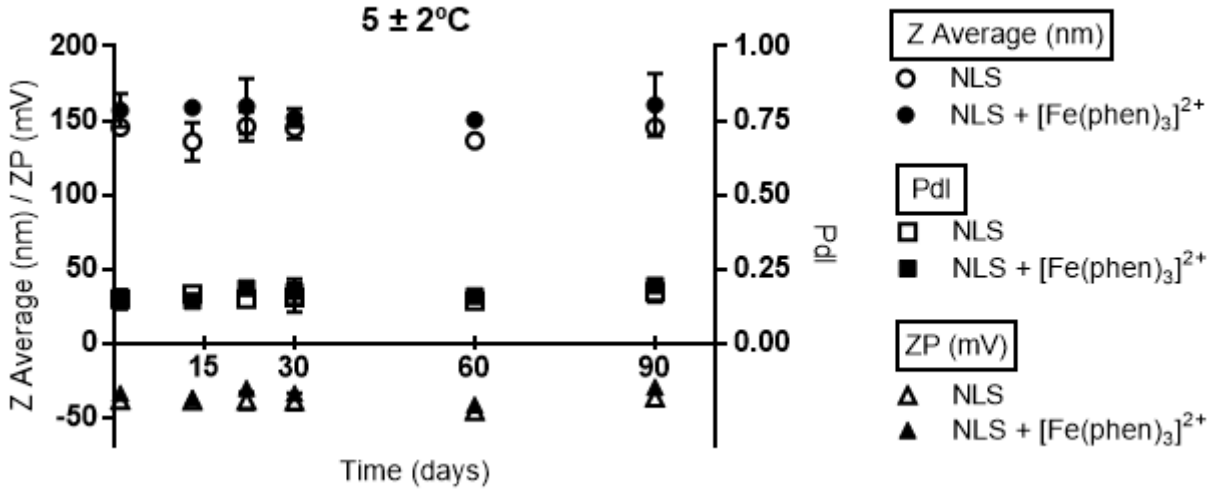

Figure 4. Values and 95% confidence interval (95% CI) of the Average particle size (Z Average), Zeta potential (ZP) and the polydispersity index (PdI), of the NLS and NLS+$[Fe(phen)_3]^{2+}$ formulations, over 90 days stored at room temperature. Three determinations of ZP and ten determinations of Z Average and PdI were performed.

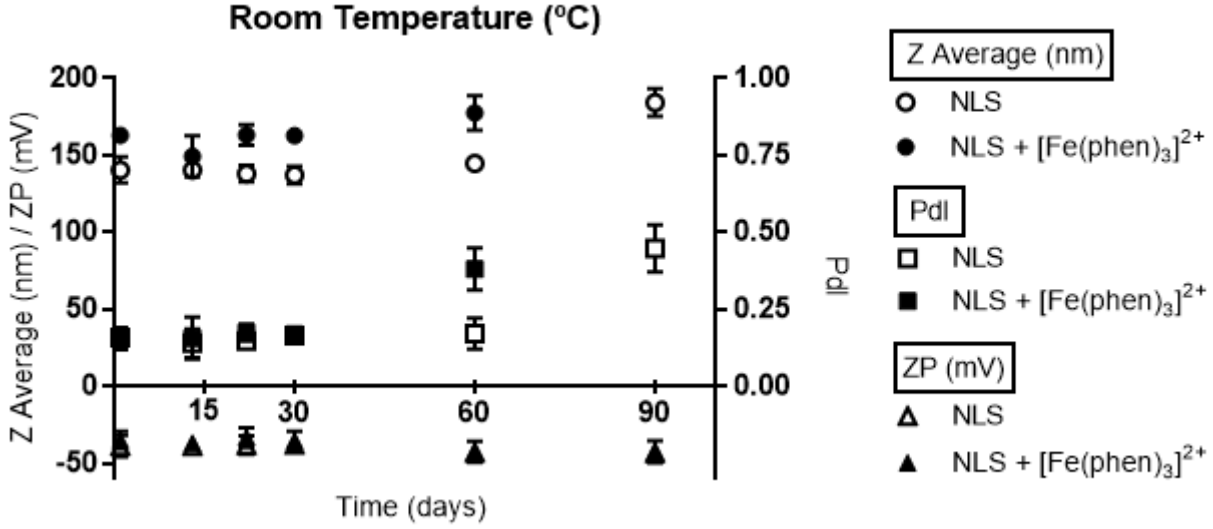

Figure 5.Values and 95% confidence interval (95% CI) of the Average particle size (Z Average), Zeta potential (ZP) and the polydispersity index (PdI), of the NLS and NLS+$[Fe(phen)_3]^{2+}$ formulations, over 90 days stored at 37ºC. Three determinations of ZP and ten determinations of Z Average and PdI were performed.

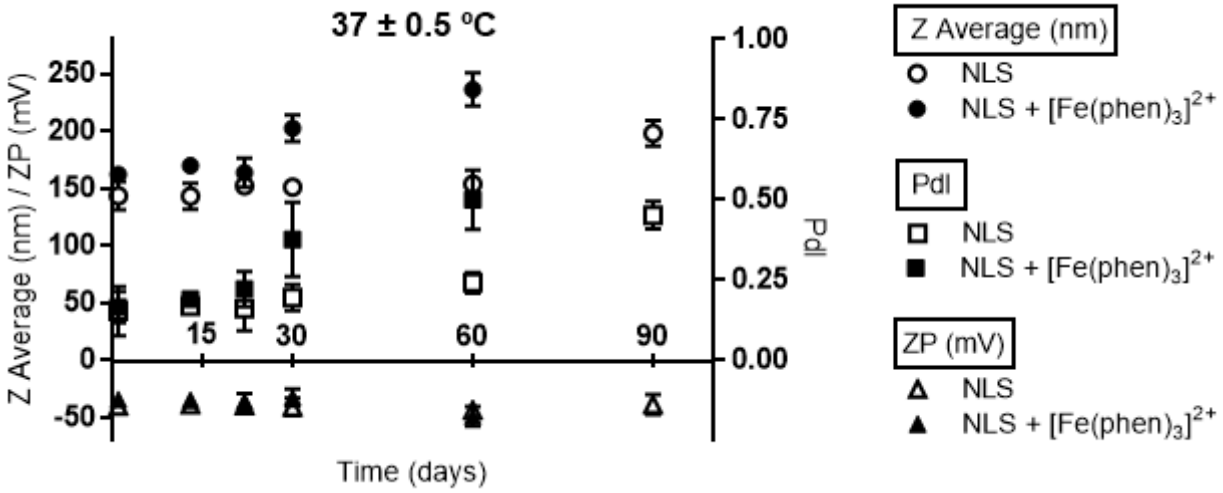

c. **Stability in culture media and solutions with different pHs**

In order to evaluate the behavior of NLS and NLS+$[Fe(phen)_3]^{2+}$ formulations at different physiological pH conditions, Z Average, PdI and ZP were analyzed. The results obtained are shown in Figure 6.

NLS and NLS+$[Fe(phen)_3]^{2+}$ showed an increase in Z Average of 4.03 nm and 3.40 nm, respectively, after 24 hours in phosphate buffer at pH 7.4. This increase in diameter is due to the presence of salt in the prepared buffer solution, which increases the solvation layer considered by the dynamic light scattering method for the determination of particle size (Moore et al. 2015). The ZP values of both formulations in phosphate buffer also highlight the interference of the buffer solution, since NLS showed a variation of ±7.03 mV and NLS+$[Fe(phen)_3]^{2+}$ of ±8.40 mV between these and their similar ones diluted in water.

After 24 hours in 0.1 M hydrochloric acid solution both formulations showed minimal increases of 0.4 nm and 0.16 nm, with no significant differences considered. The ZP values of both formulations vary from ±4.76 mV for NLS and ±5.97 mV for NLS+$[Fe(phen)_3]^{2+}$. Such behavior is due to the adsorption of ions present in the solutions, which directly interferes with the electrophoresis process performed to determine the ZP (Bhattacharjee 2016).

The PdI values for NLS and NLS+$[Fe(phen)_3]^{2+}$ in both solutions didn't show significant variation, which reinforces the stability of the particles at neutral and acidic pH solutions.

Figure 6. Mean particle size (Z Average), Polydispersity Index (PdI) and Zeta Potential (ZP) values of NLS and NLS+$[Fe(phen)_3]^{2+}$, in solutions with different pHs. 1 = Distilled water; 2 = Phosphate buffer pH 7.4; 3 = 0.1 M HCl. Three determinations of ZP and ten determinations of Z Average and PdI were performed.

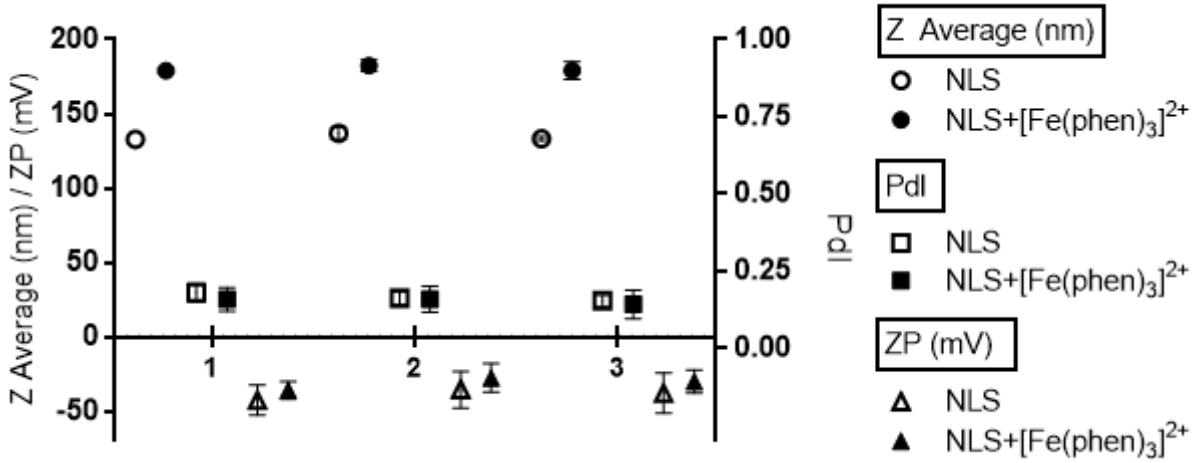

The same was performed for both formulations after their dilution in culture media DMEM high glucose and 7H9, the results are shown in Figure 7. The samples tested in both media showed an increase in Z average for NLS of approximately 15 nm and for NLS+$[Fe(phen)_3]^{2+}$ of approximately 11 nm. This increase in nanoparticle size reflects the adsorption of ions, found in solution in the culture media, onto the surface of the nanoparticles, forming larger solvation layers (Moore et al. 2015). Both formulations showed no significant variation in PdI indicating that there was no inter-particle aggregate formation. SILVA et al., 2012, observed a similar result where the solid lipid nanoparticles developed didn´t show aggregate formation in DMEM (A. C. Silva et al. 2012).

With ZP there were significant variations for NLS that went from -49.40 mV to -13.60 mV in 7H9 medium and to -7.50 mV in DMEM HIGH. The same occurred for NLS+$[Fe(phen)_3]^{2+}$ going from -38.10 mV to -10.90 mV in 7H9 and -7.80 mV in DMEM HIGH. This variation in the surface charge of the particles corresponds to the adsorption of ions present in the media (Bhattacharjee 2016). It is important to note

that both formulations, in both media, remained with negative ZP which is an interesting feature, since negatively charged particles have a lower adsorption rate of serum proteins increasing their circulation time in the body (Gera et al. 2017).

Figure 7.Mean particle size (Z Average), Polydispersity Index (PdI) and Zeta Potential (ZP) values of NLS and NLS+$[Fe(phen)_3]^{2+}$, in culture medium. 1 = Distilled water; 2 = 7H9; 3 = DMEM HIGH. Three determinations of ZP and ten determinations of Z Average and PdI were performed.

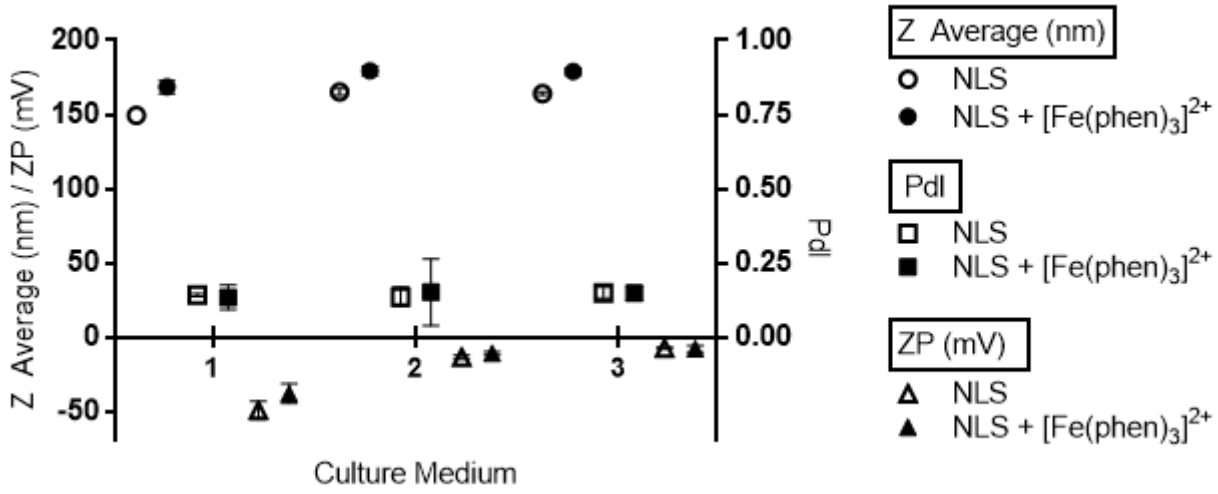

d. **Entrapment efficiency**

The NLS+$[Fe(phen)_3]^{2+}$ formulation showed average EE% of 57.72 ± 6.00 % and DL% of 0.35 ± 0.062. Both parameters are closely linked to the crystalline state of the matrix and its lipid composition (Bunjes 2011). The interaction between $[Fe(phen)_3]^{2+}$, which has a hydrophilic profile, and the lipid content of the nanostructured system plays a key role in the encapsulation and drug loading (Da Rocha et al. 2020).

Cavalcanti et al. developed nanostructured lipid carriers loaded with the hydrophilic drug zidovudine, and obtained a lower EE% (44.00 %) and a comparable DL% value (0.31 %) to the NLS+$[Fe(phen)_3]^{2+}$ (Cavalcanti et al. 2018).

Similar results of EE% (51.33 to 71.80) were obtained by Gambhire et al. where optimization of dithranol-loaded lipid nanoparticle formulations was performed followed by evaluation of the encapsulation efficiency using the ultracentrifugation method (Gambhire, Bhalekar, and Gambhire 2011).

Discussion

With the aim to end the TB epidemic, all member states of WHO adopted the End TB Strategy and the UN Sustainable Development Goals with targets set for 2030. Among the established priorities is the development of a novel drug, which can promote simpler, shorter, and more efficient treatments for TB disease (World Health Organization 2020).

In view of the results obtained by Solcia *et al.* in their work that demonstrated the great potential of the $[Fe(phen)_3]^{2+}$ against mycobacteria *in vitro*, and its bioavailability, *in vivo,* when loaded into a NLS (Solcia et al. 2021), we sought to further study the formation and stability of its incorporation into this nanostructured system and some biological aspects of $[Fe(phen)_3]^{2+}$ as its activity spectrum and resistance frequencies.

The $[Fe(phen)_3]^{2+}$ in its free form was found to have a very low rate of resistance (10^{-12}) against the H37Rv strain of *M. tuberculosis.* This fact is of great importance for therapy since one of the major challenges in fighting TB today is the emergence of high rates of bacillus resistance to available drugs (Singh et al. 2020). Another highlight is the $[Fe(phen)_3]^{2+}$ narrow spectrum of action, being highly selective against mycobacteria and leaving beneficial bacteria undamage, and therefore minimizing collateral damage to the microbiota and generating even lower possibilities for the development of bacterial resistance by species that are not affected by it (Blaser 2011; Melander, Zurawski, and Melander 2018).

When loaded into the NLS, the MIC_{90} value of $[Fe(phen)_3]^{2+}$ increases 5.6 times, compared to its free form, but it still exhibits a good inhibitory activity. The lower availability of the complex in the medium, since it is partly adhered to the nanoparticles of the lipid system, most likely causes this increase. The entrapment efficiency assay supports this result, since almost 60% of $[Fe(phen)_3]^{2+}$ is encapsulated in the particles, leaving initially only approximately 40% of the iron complex free to act against the bacilli. Besides, the stability study confirms that NLS+$[Fe(phen)_3]^{2+}$ was stable in the culture medium (7H9), used in the assay.

Particle size and morphology play an important role in the nanostructured system's performance into the biological system and may also influence their interactions with tissues and cells (Albuquerque et al. 2015; Petros and DeSimone 2010; Gera et al. 2017). The NLS and NLS+$[Fe(phen)_3]^{2+}$ particles presented a spherical shape with Z average suited for nanostructured systems, between 10 and 1000 nm (Fonseca-

Santos, Gremião, and Chorilli 2015; Gastaldi et al. 2014). It is worth mentioning that nanoparticles in the size range of 120 and 200 nm, as NLS+$[Fe(phen)_3]^{2+}$ (163 ± 0,4 nm), evade immediate liver and spleen filtration (Patel, Souto, and Singh 2013), and that the excretion rate is higher for particles larger than 200nm and particles smaller than 20–30 nm (renal excretion) (Foged et al. 2005; Gaumet et al. 2008). In general, particles sized in the nanoscale range between 50 and 250 nm have the capacity to overcome biological barriers, enhancing therapies. For this reason, they are considered promising drug delivery systems (Alexis et al. 2008).

For NLS+$[Fe(phen)_3]^{2+}$ formulation the PdI value was below 0.3, even in the different media and after 90 days at 5ºC, indicating size uniformity and monodispersed nanoparticles populations (Lopalco et al. 2015).

ZP values near to 30 mV, in modulus, of the NLS and NLS+$[Fe(phen)_3]^{2+}$ particles are considered optimum for good stabilization of a nanodispersion (C. Freitas and Müller 1998). The negative ZP values cause electric repulsion and contribute to preventing aggregation of the particles (Das and Chaudhury 2011). According to MOORE et. al., in biological media, particles that do not exhibit aggregate formation can retain a prolonged circulation half-life (Moore et al. 2015).

Due to the electrostatic repulsive interactions between the *M. tuberculosis* bacilli membrane (-2.6mV) (Ayala-Torres et al. 2014), and negatively charged particles as NLS+$[Fe(phen)_3]^{2+}$, the cellular uptake can be reduced (Chen et al. 2018). This may contribute to the understanding of the increase in the MIC_{90} value of $[Fe(phen)_3]^{2+}$ when loaded into the NLS. On the other hand, it can possibly show less toxicity to eukaryotic cells than cationic nanoparticles, which are usually associated with cell death by rupturing cell membranes (Ekambaram, Sathali, and Priyanka 2012).

Stability assays further demonstrate that NLS+$[Fe(phen)_3]^{2+}$ particles remained homogeneous in size and charge after 90 days at 5ºC and in various media, including acid solution of 0.1M HCl that is considered the simulated gastric medium (European Pharmacopoeia).

In conclusion, here, we showed new and further results of $[Fe(phen)_3]^{2+}$ indicating its specificity and its low resistance rate against *M. tuberculosis*, important finds to contribute to the search for a therapeutic drug candidate. And the obtained formulation of NLS+$[Fe(phen)_3]^{2+}$ was active against *M. tuberculosis* and presented properties like size, shape, homogeneity, surface charge and stability that makes it suitable for oral administration, meeting the need for patient compliance in the tuberculosis treatment.

Future studies must analyze the in vitro release profile, and the *in vivo* activity and safety of NLS+$[Fe(phen)_3]^{2+}$ in order to fully understand whether this combination of the $[Fe(phen)_3]^{2+}$ and the NLS has the potential to proceed as a drug candidate against TB.

References

Araujo, Victor Hugo Sousa, Patricia Bento da Silva, Isis Oliveira Szlachetka, Sebastião William da Silva, Bruno Fonseca-Santos, Marlus Chorilli, Rayane Ganassin, et al. 2020. “The Influence of NLC Composition on Curcumin Loading under a Physicochemical Perspective and in Vitro Evaluation.” *Colloids and Surfaces A: Physicochemical and Engineering Aspects* 602 (May): 125070. https://doi.org/10.1016/j.colsurfa.2020.125070.

Albuquerque, João, Catarina Costa Moura, Bruno Sarmento, and Salette Reis. 2015. “Solid Lipid Nanoparticles: A Potential Multifunctional Approach towards Rheumatoid Arthritis Theranostics.” *Molecules* 20 (6): 11103–18. https://doi.org/10.3390/molecules200611103.

Alexis, Frank, Eric Pridgen, Linda K Molnar, and Omid C Farokhzad. 2008. “Factors Affecting the Clearance and Biodistribution of Polymeric Nanoparticles.” *Molecular Pharmaceutics* 5 (4): 505–15. https://doi.org/10.1021/mp800051m.

Araujo, Victor Hugo Sousa, Patricia Bento da Silva, Isis Oliveira Szlachetka, Sebastião William da Silva, Bruno Fonseca-Santos, Marlus Chorilli, Rayane Ganassin, et al. 2020. “The Influence of NLC Composition on Curcumin Loading under a Physicochemical Perspective and in Vitro Evaluation.” *Colloids and Surfaces A: Physicochemical and Engineering Aspects* 602 (May): 125070. https://doi.org/10.1016/j.colsurfa.2020.125070.

Ayala-Torres, Carlos, Nicolás Hernández, Alejandra Galeano, Lorena Novoa-Aponte, and Carlos Y. Soto. 2014. “Zeta Potential as a Measure of the Surface Charge of Mycobacterial Cells.” *Annals of Microbiology* 64 (3): 1189–95. https://doi.org/10.1007/s13213-013-0758-y.

Bhattacharjee, Sourav. 2016. “DLS and Zeta Potential - What They Are and What They Are Not?” *Journal of Controlled Release* 235: 337–51. https://doi.org/10.1016/j.jconrel.2016.06.017.

Blaser, Martin. 2011. “Stop the Killing of Beneficial Bacteria.” *Nature* 476 (7361): 393–94. https://doi.org/10.1038/476393a.

Bunjes, Heike. 2011. “Structural Properties of Solid Lipid Based Colloidal Drug Delivery Systems.” *Current Opinion in Colloid & Interface Science* 16 (5): 405–11. https://doi.org/https://doi.org/10.1016/j.cocis.2011.06.007.

Cavalcanti, S. M.T., C. Nunes, S. A. Costa Lima, J. L. Soares-Sobrinho, and S. Reis. 2018. “Optimization of Nanostructured Lipid Carriers for Zidovudine Delivery Using a Microwave-Assisted Production Method.” *European Journal of Pharmaceutical Sciences* 122: 22–30. https://doi.org/10.1016/j.ejps.2018.06.017.

Chen, Huan, Samuel A Nyantakyi, Ming Li, Pooja Gopal, Dinah B Aziz, Tianming Yang, Wilfried Moreira, Martin Gengenbacher, Thomas Dick, and Mei L Go. 2018. “The Mycobacterial Membrane: A Novel Target Space for Anti-Tubercular Drugs.” *Frontiers in Microbiology* 9 (July): 1627. https://doi.org/10.3389/fmicb.2018.01627.

Couto, Davi Sarmento de, Rafael Nicolau Carvalho, Elisângela Braga de Azevedo, Marina Nascimento de Moraes, Patrícia Geórgia Oliveira Diniz Pinheiro, and Elaine Braga Faustino. 2014. “Fatores Determinantes Para o Abandono Do Tratamento Da Tuberculose: Representações Dos Usuários de Um Hospital Público.” *Saúde Em Debate* 38 (102): 572–81.

https://doi.org/10.5935/0103-1104.20140053.

Das, Surajit, and Anumita Chaudhury. 2011. “Recent Advances in Lipid Nanoparticle Formulations with Solid Matrix for Oral Drug Delivery.” *AAPS PharmSciTech* 12 (1): 62–76. https://doi.org/10.1208/s12249-010-9563-0.

Ekambaram, P, A. H. Sathali, and K Priyanka. 2012. “Solid Lipid Nanoparticles- A Review.” *International Journal of Applied Pharmaceutics* 2 (2): 80–102.

European Committee on antimicrobial susceptibility testing - EUCAST. 2020. “EUCAST Reading Guide for Broth Microdilution.” *Reading Guide for Broth Microdilution*. www.eucast.org.

Foged, Camilla, Birger Brodin, Sven Frokjaer, and Anne Sundblad. 2005. “Particle Size and Surface Charge Affect Particle Uptake by Human Dendritic Cells in an in Vitro Model.” *International Journal of Pharmaceutics* 298 (2): 315–22. https://doi.org/10.1016/j.ijpharm.2005.03.035.

Fonseca-Santos, Bruno, Maria Palmira Daflon Gremião, and Marlus Chorilli. 2015. “Nanotechnology-Based Drug Delivery Systems for the Treatment of Alzheimer’s Disease.” *International Journal of Nanomedicine* 10: 4981–5003. https://doi.org/10.2147/IJN.S87148.

Ford, Christopher B, Philana Ling Lin, Michael R Chase, Rupal R Shah, Oleg Iartchouk, James Galagan, Nilofar Mohaideen, et al. 2011. “Use of Whole Genome Sequencing to Estimate the Mutation Rate of Mycobacterium Tuberculosis during Latent Infection.” *Nature Genetics* 43 (5): 482–86. https://doi.org/10.1038/ng.811.

Freire, Ana Cristina, Fridrun Podczeck, João Sousa, and Francisco Veiga. 2006. “Liberação Específica de Fármacos Para Administração No Cólon Por via Oral. I - O Cólon Como Local de Liberação de Fármacos.” *Revista Brasileira de Ciencias Farmaceuticas/Brazilian Journal of Pharmaceutical Sciences* 42 (3): 319–35. https://doi.org/10.1590/s1516-93322006000300003.

Freitas, Chrysantha, and Rainer H Müller. 1998. “Effect of Light and Temperature on Zeta Potential and Physical Stability in Solid Lipid Nanoparticle (SLN^{TM}) Dispersions.” *International Journal of Pharmaceutics* 168 (2): 221–29. https://doi.org/https://doi.org/10.1016/S0378-5173(98)00092-1.

Freitas, Eduardo Sinesio De, Patricia Bento Da Silva, Marlus Chorilli, Alzir Azevedo Batista, Érica De Oliveira Lopes, Monize Martins Da Silva, Clarice Queico Fujimura Leite, and Fernando Rogério Pavan. 2014. “Nanostructured Lipid Systems as a Strategy to Improve the in Vitro Cytotoxicity of Ruthenium(II) Compounds.” *Molecules* 19 (5): 5999–6008. https://doi.org/10.3390/molecules19055999.

Gambhire, Makarand Suresh, Mangesh Ramesh Bhalekar, and Vaishali Makarand Gambhire. 2011. “Statistical Optimization of Dithranol-Loaded Solid Lipid Nanoparticles Using Factorial Design.” *Brazilian Journal of Pharmaceutical Sciences* 47 (3): 503–12. https://doi.org/10.1590/S1984-82502011000300008.

Gao, Enjun, Na Sun, Shaozhong Zhang, Yuqing Ding, Xue Qiu, Yang Zhan, and Mingchang Zhu. 2016. “Synthesis, Structures, Molecular Docking, Cytotoxicity and Bioimaging

Studies of Two Novel Zn(II) Complexes." *European Journal of Medicinal Chemistry* 121: 1–11. https://doi.org/https://doi.org/10.1016/j.ejmech.2016.05.013.

Gastaldi, Lucia, Luigi Battaglia, Elena Peira, Daniela Chirio, Elisabetta Muntoni, Ilaria Solazzi, Marina Gallarate, and Franco Dosio. 2014. "Solid Lipid Nanoparticles as Vehicles of Drugs to the Brain: Current State of the Art." *European Journal of Pharmaceutics and Biopharmaceutics : Official Journal of Arbeitsgemeinschaft Fur Pharmazeutische Verfahrenstechnik e.V* 87 (3): 433–44. https://doi.org/10.1016/j.ejpb.2014.05.004.

Gaumet, Marie, Angelica Vargas, Robert Gurny, and Florence Delie. 2008. "Nanoparticles for Drug Delivery: The Need for Precision in Reporting Particle Size Parameters." *European Journal of Pharmaceutics and Biopharmaceutics : Official Journal of Arbeitsgemeinschaft Fur Pharmazeutische Verfahrenstechnik e.V* 69 (1): 1–9. https://doi.org/10.1016/j.ejpb.2007.08.001.

Gera, Meeta, Neelesh Sharma, Mrinmoy Ghosh, Do Luong Huynh, Sung Jin Lee, Taesun Min, Taeho Kwon, and Dong Kee Jeong. 2017. "Nanoformulations of Curcumin: An Emerging Paradigm for Improved Remedial Application." *Oncotarget* 8 (39): 66680–98. https://doi.org/10.18632/oncotarget.19164.

Gerasimova, Tatiana P., and Sergey A. Katsyuba. 2013. "Bipyridine and Phenanthroline IR-Spectral Bands as Indicators of Metal Spin State in Hexacoordinated Complexes of Fe(Ii), Ni(Ii) and Co(Ii)." *Dalton Transactions* 42 (5): 1787–97. https://doi.org/10.1039/c2dt31922e.

Homayun, Bahman, Xueting Lin, and Hyo-Jick Choi. 2019. "Challenges and Recent Progress in Oral Drug Delivery Systems for Biopharmaceuticals." *Pharmaceutics* 11 (3): 129. https://doi.org/10.3390/pharmaceutics11030129.

Ignatius, Elisa H., and Kelly E. Dooley. 2019. "New Drugs for the Treatment of Tuberculosis." *Clinics in Chest Medicine* 40 (4): 811–27. https://doi.org/10.1016/j.ccm.2019.08.001.

Laouini, Abdallah, Konstantinos P. Koutroumanis, Catherine Charcosset, Stella Georgiadou, Hatem Fessi, Richard G. Holdich, and Goran T. Vladisavljević. 2013. *PH-Sensitive Micelles for Targeted Drug Delivery Prepared Using a Novel Membrane Contactor Method*. *ACS Applied Materials and Interfaces*. Vol. 5. https://doi.org/10.1021/am4018237.

Lee, C. N., and L. B. Heifets. 1987. "Determination of Minimal Inhibitory Concentrations of Antituberculosis Drugs by Radiometric and Conventional Methods." *American Review of Respiratory Disease* 136 (2): 349–52. https://doi.org/10.1164/ajrccm/136.2.349.

Lopalco, Antonio, Hazem Ali, Nunzio Denora, and Erik Rytting. 2015. "Oxcarbazepine-Loaded Polymeric Nanoparticles: Development and Permeability Studies across in Vitro Models of the Blood-Brain Barrier and Human Placental Trophoblast." *International Journal of Nanomedicine* 10: 1985–96. https://doi.org/10.2147/IJN.S77498.

Melander, Roberta J, Daniel V Zurawski, and Christian Melander. 2018. "Narrow-Spectrum Antibacterial Agents." *MedChemComm* 9 (1): 12–21. https://doi.org/10.1039/C7MD00528H.

Ministério da Saúde Brasil. 2017. *Brasil Livre Da Tuberculose: Plano Nacional Pelo Fim*

Da Tuberculose Como Problema de Saúde Pública. *Secretaria de Vigilância Em Saúde. Departamento de Vigilância Das Doenças Transmissíveis.* http://bvsms.saude.gov.br/bvs/publicacoes/brasil_livre_tuberculose_plano_nacional.pdf.

Moore, Thomas L., Laura Rodriguez-Lorenzo, Vera Hirsch, Sandor Balog, Dominic Urban, Corinne Jud, Barbara Rothen-Rutishauser, Marco Lattuada, and Alke Petri-Fink. 2015. "Nanoparticle Colloidal Stability in Cell Culture Media and Impact on Cellular Interactions." *Chemical Society Reviews* 44 (17): 6287–6305. https://doi.org/10.1039/c4cs00487f.

Müller, R H, M Radtke, and S A Wissing. 2002. "Solid Lipid Nanoparticles (SLN) and Nanostructured Lipid Carriers (NLC) in Cosmetic and Dermatological Preparations." *Advanced Drug Delivery Reviews* 54 Suppl 1 (November): S131-55. https://doi.org/10.1016/s0169-409x(02)00118-7.

Nasiruddin, Mohammad, Md Kausar Neyaz, and Shilpi Das. 2017. "Nanotechnology-Based Approach in Tuberculosis Treatment." *Tuberculosis Research and Treatment* 2017: 4920209. https://doi.org/10.1155/2017/4920209.

Orvig, Chris, and Michael J Abrams. 1999. "Medicinal Inorganic Chemistry: Introduction." *Chemical Reviews* 99 (9): 2201–4. https://doi.org/10.1021/cr980419w.

Palomino, Juan-Carlos, Anandi Martin, Mirtha Camacho, Humberto Guerra, Jean Swings, and Françoise Portaels. 2002. "Resazurin Microtiter Assay Plate: Simple and Inexpensive Method for Detection of Drug Resistance in Mycobacterium Tuberculosis." *Antimicrobial Agents and Chemotherapy* 46 (8): 2720–22. https://doi.org/10.1128/AAC.46.8.2720-2722.2002.

Patel, Medha, Eliana B Souto, and Kamalinder K Singh. 2013. "Advances in Brain Drug Targeting and Delivery: Limitations and Challenges of Solid Lipid Nanoparticles." *Expert Opinion on Drug Delivery* 10 (7): 889–905. https://doi.org/10.1517/17425247.2013.784742.

Petros, Robby A, and Joseph M DeSimone. 2010. "Strategies in the Design of Nanoparticles for Therapeutic Applications." *Nature Reviews. Drug Discovery* 9 (8): 615–27. https://doi.org/10.1038/nrd2591.

Rabahi, Marcelo Fouad, José Laerte, Silva Júnior, Anna Carolina, Galvão Ferreira, Daniela Graner Schuwartz Tannus-silva, Marcus Barreto Conde, and Faculdade De Medicina. 2017. "Tratamento Da Tuberculose." *Jornal Brasileiro de Pneumologia* 43 (5): 472–86.

Rieux, Anne des, Virginie Fievez, Maryam Momtaz, Christophe Detrembleur, Maria Alonso-Sande, Jan Van Gelder, Annick Cauvin, Yves Jacques Schneider, and Véronique Préat. 2007. "Helodermin-Loaded Nanoparticles: Characterization and Transport across an in Vitro Model of the Follicle-Associated Epithelium." *Journal of Controlled Release* 118 (3): 294–302. https://doi.org/10.1016/j.jconrel.2006.12.023.

Rocha, Márcia Cristina Oliveira Da, Patrícia Bento Da Silva, Marina Arantes Radicchi, Bárbara Yasmin Garcia Andrade, Jaqueline Vaz De Oliveira, Tom Venus, Carolin Merker, Irina Estrela-Lopis, João Paulo Figueiró Longo, and Sônia Nair Báo. 2020. "Docetaxel-Loaded Solid Lipid Nanoparticles Prevent Tumor Growth and Lung Metastasis of 4T1 Murine Mammary Carcinoma Cells." *Journal of Nanobiotechnology* 18 (1): 1–20. https://doi.org/10.1186/s12951-020-00604-7.

Santos Fernandes, Guilherme Felipe Dos, Paula Carolina De Souza, Elsa Moreno-Viguri, Mery Santivañez-Veliz, Rocio Paucar, Silvia Pérez-Silanes, Konstantin Chegaev, et al. 2017. “Design, Synthesis, and Characterization of N-Oxide-Containing Heterocycles with in Vivo Sterilizing Antitubercular Activity.” *Journal of Medicinal Chemistry* 60 (20): 8647–60. https://doi.org/10.1021/acs.jmedchem.7b01332.

Silva, A C, A Kumar, W Wild, D Ferreira, D Santos, and B Forbes. 2012. “Long-Term Stability, Biocompatibility and Oral Delivery Potential of Risperidone-Loaded Solid Lipid Nanoparticles.” *International Journal of Pharmaceutics* 436 (1–2): 798–805. https://doi.org/10.1016/j.ijpharm.2012.07.058.

Silva, José Alexsandro da, Davi Pereira de Santana, Danilo Galindo César Bedor, Valeria Ferreira da Costa Borba, Ana Amélia Moreira Lira, and Eryvaldo Socrates Tabosa do Egito. 2009. “Estudo de Liberação e Permeação in Vitro Do Diclofenaco de Dietilamônio Em Microemulsão Gel-Like.” *Química Nova* 32 (6): 1389–93. https://doi.org/10.1590/S0100-40422009000600005.

Silva, Patricia B. Da, Eduardo Sinésio De Freitas, Mariana Cristina Solcia, Paula Carolina De Souza, Monize Martins Da Silva, Alzir Azevedo Batista, Carlos E. Eismann, et al. 2018. “A Nanostructured Lipid System to Improve the Oral Bioavailability of Ruthenium(II) Complexes for the Treatment of Infections Caused by Mycobacterium Tuberculosis.” *Frontiers in Microbiology* 9 (DEC): 1–11. https://doi.org/10.3389/fmicb.2018.02930.

Silva, Patricia B. da, Paula C. de Souza, Giovana Maria Fioramonti Calixto, Erica de O. Lopes, Regina C.G. Frem, Adelino V.G. Netto, Antonio E. Mauro, Fernando R. Pavan, and Marlus Chorilli. 2016. “In Vitro Activity of Copper(II) Complexes, Loaded or Unloaded into a Nanostructured Lipid System, against Mycobacterium Tuberculosis.” *International Journal of Molecular Sciences* 17 (5). https://doi.org/10.3390/ijms17050745.

Silva, Pollyanna da Fonseca, Germano Silva Moura, Arlene de Jesus Mendes Caldas, Pollyanna da Fonseca Silva, Germano Silva Moura, and Arlene de Jesus Mendes Caldas. 2014. “Fatores Associados Ao Abandono Do Tratamento Da Tuberculose Pulmonar No Maranhão, Brasil, No Período de 2001 a 2010.” *Cadernos de Saúde Pública* 30 (8): 1745–54. https://doi.org/10.1590/0102-311X00124513.

Singh, R, S P Dwivedi, U S Gaharwar, R Meena, P Rajamani, and T Prasad. 2020. “Recent Updates on Drug Resistance in Mycobacterium Tuberculosis.” *Journal of Applied Microbiology* 128 (6): 1547–67. https://doi.org/https://doi.org/10.1111/jam.14478.

Solcia, Mariana Cristina, Débora Leite Campos, Júlia Araújo Grecco, Caio Sander Paiva Silva, Patrícia Bento da Silva, Isabel Cristiane da Silva, Ana Paula Balduino da Silva, et al. 2021. “Growth-Inhibitory Effects of Tris-(1,10-Phenanthroline) Iron (II) against Mycobacterium Tuberculosis in Vitro and in Vivo.” *Tuberculosis* 128 (April): 1–8. https://doi.org/10.1016/j.tube.2021.102087.

Toledo, Lucas de Alcântara Sica de, Hélen Cássia Rosseto, and Marcos Luciano Bruschi. 2018. “Iron Oxide Magnetic Nanoparticles as Antimicrobials for Therapeutics.” *Pharmaceutical Development and Technology* 23 (4): 316–23. https://doi.org/10.1080/10837450.2017.1337793.

Vasava, Mahesh S, Manoj N Bhoi, Sanjay K Rathwa, Mayuri A Borad, Sneha G Nair, and

Hitesh D Patel. 2017. “Drug Development against Tuberculosis: Past, Present and Future.” *Indian Journal of Tuberculosis* 64 (4): 252–75. https://doi.org/https://doi.org/10.1016/j.ijtb.2017.03.002.

Wang, Xiaoyan, Gan Jia, Yuting Yu, Yanfang Gao, Wen Zhang, Hong Wang, Zhenzhu Cao, and Jinrong Liu. 2015. “A New Homogeneous Electrocatalyst for Electrochemical Carbonylation of Methanol to Dimethyl Carbonate” 38 (3): 298–302.

Wellington, Samantha, and Deborah T Hung. 2018. “The Expanding Diversity of Mycobacterium Tuberculosis Drug Targets.” *ACS Infectious Diseases* 4 (5): 696–714. https://doi.org/10.1021/acsinfecdis.7b00255.

World Health Organization, (WHO). 2020a. *WHO Report on TB 2020*. *Who*. Vol. 1. https://www.who.int/publications-detail-redirect/9789240013131.

World Health Organization (WHO). 2021. *Meeting Report of the WHO Expert Consultation on the Definition of Extensively Drug-Resistant Tuberculosis*. http://apps.who.int/bookorders.